Effectiveness of an ADAM10 inhibitor as a radio-sensitizer to improve the treatment of cervical cancer

M Rasakanya

orcid.org/0000-0002-6092-055X

Mini-Dissertation submitted *in partial fulfillment* of the requirements for the Master's degree in Applied *Radiation Science and Technology*
at the North-West University

Supervisor: Prof Manny Mathuthu
Co-Supervisor: Dr Julie Bolcaen – (iThemba LABS)

Graduation: November 2022
Student number: 26505584

Table of Contents

List of figures

List of tables

Acronyms and abbreviations

ACC	Adenocarcinoma carcinoma cells
ADAM	A disintegrin and metalloproteinase
ASC	Adeno-squamous carcinoma
ATM	Ataxia-telangiectasia mutated
CCA	Clear cell adenocarcinoma
CCSCSs	Cervical cancer stem cells
CSA	Colony survival assay
CSC	Cancer stem cells
CT	Computed tomography
DDR	DNA damage response
DES	Diethylstilbestrol
EBRT	External beam radiation therapy
FIGO	International Federation of Obstetrics and Gynecology
GSI	Γ-secretase inhibitor
HPV	Human papillomavirus
IL-11	Interleukin-11
IMRT	Intensity-modulated radiotherapy
IR	Irradiation
LN	Lymph node
ERK/MAPK	Mitogen-activated protein kinases
MMP	Matrix metalloproteinase
MRI	Magnetic resonance imaging

NAAT	Nucleic acid amplification test
NICD	Notch intercellular domain
OS	Overall survival
PARP	Poly adenosine diphosphate-ribose polymerase
PFS	Progression-free survival
PI3K	Phosphoinositide 3-kinases
ROS	Reactive oxygen species
RR	Radiation response
RT	Radiation therapy
SCC	Squamous carcinoma cells
SD	Standard deviation
SF	Survival fraction
STD	Sexual transmitted disease
TI	Therapeutic index
TIMPs	Tissue inhibitors of metalloproteinases
TNF	Tumor necrosis factor
VEGF	Vascular endothelial growth factor
WHO	World Health Organization

Acknowledgment

I would like to thank my supervisor Dr. Julie Bolcaen, who guided me throughout the experiments along with the assistance of Dr. Shankari Nair, and PhD student/lab technician Xanthene Muller and iThemba LABS for giving me the opportunity to do this research under the financial assistance of my SAINTS scholarship.

Declaration

This research was done and completed by Mokokobale Rasakanya under the supervision of the radiation biophysics division of iThemba LABS and North-West University Mafikeng Campus.

Abstract

Cervical cancer is the third most common type of cancer in women in developing countries with around 570 000 cases and 311 000 deaths recorded worldwide in 2018. In South Africa, over 90% of the cases are related to human papillomavirus (HPV) infection and annually, 5 743 new cases and 3 027 deaths are registered. Surgery, external beam therapy and chemotherapy are the standard treatments of cervical cancer, where combined therapy increases the survival rate of the patients. Though early stage cancer is curable, the median overall survival in cases of an advanced, recurrent disease is just over a year. Due to a lack of regular screening in developing countries, cervical cancer is often only detected at an advanced stage and therapy is not always available. Thus, there is an urgent need to improve current treatments and develop new strategies to treat cervical cancer. The goal of this dissertation was to determine the effectiveness of a disintegrin and metalloproteinase (ADAM10) inhibitor as a radiosensitizer for the treatment of cervical cancer. Inhibition of ADAM10 has been considered as a promising novel targeted cancer treatment strategy due to its role in the shedding off of a number of substrates that drive cancer progression. In addition, due to its role in the radiation response (RR) and Notch signaling pathway, blocking ADAM10 could enhance the effectiveness of radiation therapy (RT). In this dissertation, we successfully optimized the migration, apoptosis and invasion assay. Based on our results, we could conclude that the deregulation of ADAM10 activity by GI254023X (GI) had an effect on the migration of the Hela cells since it slowed down the gap closure. However, only one repeat was performed due to COVID 19 restriction. In contrast, no effect of GI on the invasion of the cervical cancer cells was seen. Results of the CSA assay were unclear and need to be repeated in the future to make a conclusion on the effect of GI on colony formation. Finally, a trend was seen to increase the apoptosis of Hela cells when control was compared to 2Gy+GI, which was not visible when control was compared with 2Gy only. However, when 2Gy was compared to 2Gy+GI, no significant differences were seen in living or apoptotic cells. Combined therapy of GI and RT had no increased inhibitory effects compared to single therapy in any of the

assays studied. Therefore, based on our results, we could not conclude that GI254023X functions as a radiosensitizer for cervical cancer.

Chapter 1: Introduction and problem statement

1.1. Cervical cancer

1.1.1. What is cancer?

The human body is made up of more than a billion genes based on amino acids that are arranged in a manner to code for certain organs and tissues, along with cellular functions (NCI, 2021a). A sudden change in the genetic makeup or mutation can lead to the development and uncontrolled growth of cells within the human body (Genomes Project et al., 2015). This sudden appearance of cancer is still a mystery in science whether its appearance is due to genes, which was passed on from parent to child or environmental factors, such as climate change or harmful chemicals that the individual has been exposed to during his/her life time (Weinberg, 1996). However, a mutation does not always result in the formation of cancer, some of these genetic changes can be fixed by the organisms since the cell cycle has a DNA repair ability that can correct changes in DNA. Some mutations that occurred through the life cycle of cells have helped in the evolution of humans and most of these mutations are not harmful, such as silent mutations (Genomes Project et al., 2015). However, in the case that the mutation is cancerous, an uncontrolled growth of cells within the human body results, which may form tumors and can disrupt normal functions of the human body (Bailar and Gornik, 1997).

There are evidences that showed that the transformation of normal human cells into malignant cancer cells is a multi-step process that reflects genetic alternations (Hanahan and Weinberg, 2000). If a tumor develops, some tumors will be non-cancerous known as a benign tumor while some will be cancerous, which can be distinguished by the ability to spread into or invade nearby tissues and travel to distant places within the body to form new tumors, resulting in the formation of metastasis (NCI, 2021b). Cancer is a disease that often can be treated, where people after a successful treatment, can still carry on with their lives. Therefore, the increase in deaths due to cancer is a problem in the world today, which could be ameliorated.

In developed countries, cancer is mostly seen in older people around the age of 60 and this is because as we get older, there is an increased number of cell damages and a decreased number of cell repairs, leading to the development of more mutations in the body. These mutations can grow and become uncontrolled tumors that can spread to other parts of the body (White et al., 2014). There are six biological capabilities acquired during the multistep development of human tumors, which have been identified as the hallmarks of cancer. These include sustaining proliferative signaling, evading growth suppressors, resisting cell death, enabling replicative immortality, inducing angiogenesis, and activating invasion and metastasis. In addition, two characteristics facilitate acquisition of these cancer hallmarks: genome instability and inflammation (Hanahan and Weinberg, 2011).

1.1.2. What is cervical cancer?

Cervical cancer is the development of a malignant tumor in the cervix that occurs when there is a change in DNA arrangement or structures of the cells that makeup the cervix. This results in the accumulation of abnormal cells known as a tumor, which may move to other parts of the body. For the anatomy of the female reproductive system, refer to Figure 1. The organs in the female reproductive system include the uterus, ovaries, fallopian tubes, cervix, and vagina. The uterus has a muscular outer layer called the myometrium and an inner lining called the endometrium (Chen et al., 2011, NCI, 2021b).

Cervical cancer is the third most common cancer in women in the world and the second most common cancer affecting Southern African women after breast cancer. Cervical cancer remains the most lethal cancer in women worldwide and targets the younger population (Khan et al., 2016, CANCSA, 2016). Cervical cancer has become a problem in women in developing countries due to the lack of screening that woman must go through every year, which is very rare when women have little knowledge on vaginal health. When dealing with cervical cancer, early detection has a major effect on the prognosis and even the cost of the treatment, which depends on the stage of the cancer

and type of treatment offered (Mishra et al., 2011, NCI, 2021b, Olivares-Urbano et al., 2020).

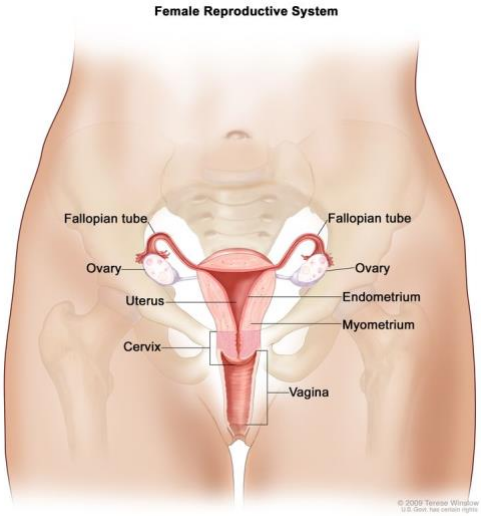

Figure 1**:** Anatomy of the female reproductive system (NCI, 2021a).

1.1.3. Up-rise of cervical cancer in developing countries

Vaginal health is a topic that is not talked about with young women in developing countries as adults see any of these topics as a taboo, creating misconception and fear in young woman (Palmeira-de-Oliveira et al., 2014, Kuhle et al., 2021). Women in developing countries fall prey to myths that are created by elders about virginal health, causing them to follow certain practices without a doctor supervision, which can affect them later in life. As a result, these women never consult doctors or go for routine checkups that every woman should for go after starting their periods (Klein et al., 2018, Kalyanaraman, 2017). By looking into low and middle-income families, in these countries, such as South Africa, it can be seen that poverty has caused a lack of information regarding cervical cancer. Cancer is a disease that is not new to the world and is not widely talked about in developing countries. The rise of deaths due to cancer has led to people questioning its sudden appearance in these countries yet one of the major reasons is lack of medical health programs, such as screening and prevention for cervical cancer programs alongside poverty, socio-religious and cultural barriers, which restrict them from testing (Dahiya et al., 2016, Catarino et al., 2015).

When looking at the health of people in developing countries, one of the major diseases that people focus on is HIV, which is important to educate people about, but they tend to forget that they are other sicknesses that can also affect their lives. People in developing countries are dying due to HIV and AIDs but with the help of organizations and government funds, people are learning to accept HIV and are following healthy sexual practices that ensure their safety (Antabe and Mkandawire, 2020). This, on the other hand, cannot be said for cancer due to the lack of knowledge and understanding of what cancer is in developing countries. Unlike HIV, certain cancer types can be successfully treated and cured but because of the lack of information and medical facilities, the death rate is high (Dahiya et al., 2016).

Cervical cancer is not a sexually transmitted disease (STD) but patients, who have tested positive for chlamydia and HPV have a higher risk of developing cancer if left untreated. The high numbers of cervical cancer in developing countries is also attributed to early sexual activities, having multiple partners, thus increasing the chances of getting STDs, infrequent use of condoms, having multiple pregnancies with chlamydia association and immunosuppression with HIV, which is related to a higher risk of HPV infection (Ibeanu, 2011). One of the reasons why a lot of women in developing countries are dying of cervical cancer is because during the early stages of cervical cancer development, there are no direct symptoms that can indicate that one has cancer and if symptoms appear, which are associated with cervical cancer, it can be misleading, causing them to seek treatment only at an advanced stage of cervical cancer (team, 2020a, CANCSA, 2016, WHO, 2021).

1.1.4. Different stages and symptoms of cervical cancer

a. Stages of cervical cancer

The staging of cervical cancer is determined by how far the cancer has spread within the cervix and the body, based on the size of the tumor and how much area within the pelvis is affected. Refer to Figure 2 and Table 1 for staging based on the International Federation of Obstetrics and Gynecology (FIGO). The stage of cervical cancer is

determined during the first testing and will not change even if a recurrence of cervical cancer occurs.

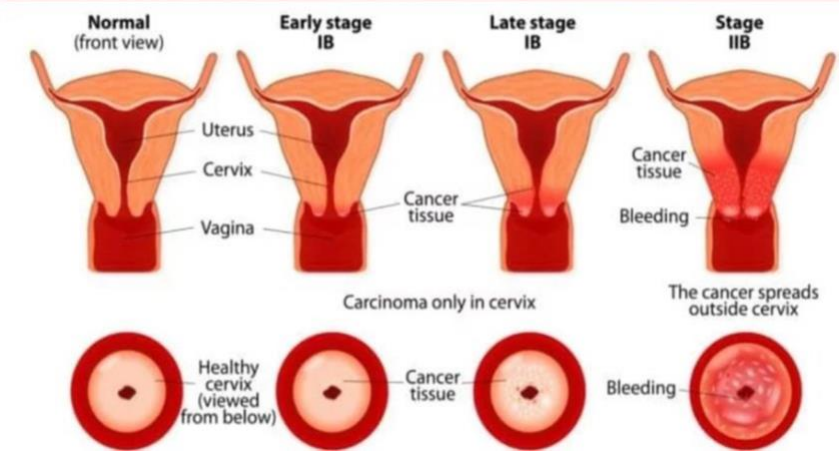

Figure 2**:** Stages of cervical cancer
(Mustafa et al., 2020).

Table 1**:** Cervical cancer stages and development
(Bhatla et al., 2019).

Stage			**Growth site, length, and invasion**
Stage I			Cervical cancer that has developed from the cervix due to mutations and starts to spread from the cervix lining into deeper tissues, it has not spread to other parts of the body and only found in the uterus
	Stage IA		In this stage the cancer can only be detected by biopsy and imaging can be done to determine the size of the tumor
		Stage IA1	This stage is when the cancer has spread to less than an area of 3-mm-deep within the uterus
		Stage IA2	This stage is when the cancer is has spread to areas 3 mm but less than 5 mm deeper in the uterus
	Stage IB		Size of tumor is larger compared to stage IA but it is still only located in the cervix
		Stage IB1	Tumor is less than 4 mm deep and width is less than 2 cm
		Stage IB2	Tumor is 2 cm deep and less than 4 cm wide
Stage II			Tumor has spread to nearby areas such as the vagina and other tissues near the cervix but only located in the pelvic areas
	Stage IIA		Tumor spread to the upper layer of the vagina
		Stage IIA1	Tumor is less than 4 cm in width
		Stage IIA2	Tumor is more than 4 cm in width
	Stage IIB		Tumor has spread to the parametrical area but not located in the pelvic wall
Stage III			Tumor is in the lower third of the vagina. It has spread to the pelvic wall and caused kidney to become enlarged.
	Stage IIIA		Tumor is in the lower third of the vagina but not in the pelvic wall
	Stage IIIB		Tumor is in the pelvic wall and now affects the function of the kidney
Stage IV			Tumor is beyond true pelvis or clinically involves mucosa of bladder or rectum.
	Stage IVA		Tumor has spread to the bladder or the rectum but not to distance organs
	Stage IVB		Tumor has metastasis and spread to distance organs

b. Symptoms of cervical cancer

i. Early-stage cervical cancer symptoms

- Pain when having sex
- An unusual virginal bleeding that can occur after sex, between your periods, after menopause or after a pelvic exam
- Unusual virginal discharge

ii. Symptoms after the cancer has spread

- Swelling legs
- Urination problems
- Having bowel movements
- Blood in the urine

1.1.5. Risk factors for the development of cervical cancer

The development of cervical cancer cannot be directly linked to a specific cause as the human body reacts and responds in different manners to certain factors. These factors are only seen as risks that can increase the likelihood of developing cervical cancer as there is no clinical trial to prove such claims, unlike in the case of diethylstilbestrol (DES), which was a non-steroidal estrogen prescribed oral medicine given to pregnant women to help them in the prevention of miscarriages in the 1940s to the 1970s (Al Jishi and Sergi, 2017). The genetic effect that has resulted in the use of DES has resulted in infertility, early menopause and even cancer for these women and their offspring, which have been seen to be passed on to the next generation (Titus et al., 2019). However, because not all the women and offspring of DES developed cervical cancer, it could not be stated as a cause but a risk factor, even with the strong link between DES and clear cell adenocarcinoma (CCA) that develops in the vagina and cervix of these women (Troisi et al., 2007).

This can also be said for HPV. There are more than 100 types of HPV with about 15 at least that are known to be carcinogenic but only two types of HPV, specifically type 16 and type 18 are known to have a 70 percentage chance of causing cervical cancer (Burger et al., 2017). HPV is a sexually transmitted disease that can cause the

formation of genital warts or pre-cancerous lesion, which could possibly develop into cancer. Cervical cancer might be known as one of the diseases that are related to HPV as most cases were corresponding to patients, who have been infected with HPV, but taking into consideration that it could take years for cervical cancer to develop and spread within the human body, which makes it harder to determine its real cause (Wardak, 2016).

a. List of risk factors for the development of cervical cancer include:

- Having many sexual partners
- Early sexual activity
- Sexually transmitted diseases (HPV)
- A weakened immune system
- Smoking
- Exposure to miscarriage prevention drug (DES)

1.1.6. Different types of cervical cancer and metastasis

Cervical cancer is divided into different groups based on the initial growth of the cancer, which is known as squamous carcinoma cells (SCC) and adenocarcinoma carcinoma cells (ACC). The SCC is a cancer that originates at the thin flat line of cells that are located at the bottom of the cervix and ACC is a cancer that originates at the upper layer of the cervix, where glandular cells are located (Hilal, 2016, team, 2020b). There are some rare cases, where patients would have a mixture of the two different types of cancer, also called adeno-squamous carcinoma (ASC) (Stolnicu, 2019). Cervical cancer can also be grouped based on how it metastasizes in the body. If the cancer spreads through the bloodstream, it can affect the bones and soft tissues, which is known as hematogenous metastasis. When the cancer spreads through the lymphatic system, it can spread to the lungs, breast, colon, etc. which is known as lymphatic metastasis or it can spread through body walls, reaching abdominal areas, which is known as transcoelomic metastasis (Univerisity, 2018).

- Squamous carcinoma cell (SCC)
- Adenocarcinoma carcinoma cell (ACC)
- Adeno-squamous carcinoma cells (ASC)
- Hematogenous metastasis
- Lymphatic metastasis
- Transcoelomic metastasis

1.2. Cervical cancer screening

The guidelines of the South African Department of Health for screening of cervical cancer provides three target groups based on the level of risk of the individual, see Tables 2 and 3. The Policy Statement 3 states that all women from 30-50 years of age must be screened for cervical cancer based on the recommendation provided by the South Africa Department of Health (Health, 2017).

Table 2**:** Screening recommendation by the department of health of South Africa (Health, 2017).

Target	Recommendation	Age	Screening interval
General or low risk population	Women who have never been screened and have not been infected with HIV.	30-50	Every 10 years starting at the age of 30. If abnormality is found than screening interval is every 3 years.
HIV-positive or high-risk population	Women, who are HIV-positive have received an organ transplant, have a disease that suppresses their immune system or those on any chronic immune suppressing treatment.	From the age the patient has been diagnosed with stated medical condition	Every 3 year of their life stating when after being diagnosed of stated condition
Symptomatic women	Women with symptoms of cervical cancer or those that have been infected with STI	From the age the patient has been diagnosed with stated medical condition	Every 3 years of their life stating when after being diagnosed of stated condition

The guidelines for cervical cancer screening may be different for each country but also under the guidelines of the World Health Organization (WHO), it can be said that screening for cervical cancer for women is grouped based on the health of the woman, where the presence of STD such as HPV or HIV, having pre-cancer or women with histological confirmation are considered high risk and regular screening for early detection of cervical cancer is advised. Based on the WHO guideline, women who have tested positive for HPV, should be tested every 5 to 10 years starting from the age of 30, while women, who are HIV positive need regular screening every 3 to 5 years once they reach the age of 25. During these screenings and when an abnormality is detected, further tests are performed to determine if the tumor is cancerous, stage, location and which organs are affected by the tumor (WHO, 2021).

Table 3**:** Three approaches to cervical cancer screening and future tests (WHO, 2021).

Type of test	**Procedure**	**Based on**
Visual inspection	Visual inspection with acetic acid or with Lugol's iodine	Naked eye Magnified by colposcopy or camera
	Automated visual evaluation of images	
Cytologic	Conventional Pap smear	
	Liquid-based cytology	
	Dual staining to identify p16 and ki-67	
Molecular	Nucleic acid amplification test (NAAT)	High-risk HPV DNA/ NAAT mRNA
	DNA methylation	
	Protein biomarker	HPV antibodies Oncoprotein

There are multiply steps that are taken into consideration when determining if a patient has cervical cancer. Traditional method of screening for cervical cancer is by cytology, where a pap test is performed and when the test is positive, a biopsy is done. The biopsy is done to determine the presences of lesions and do histological examinations. If these tests are done during the early stage, there is a higher survival rate for the patient. There is a development of new techniques for cervical cancer screening based on visual inspection, molecular testing and cytologic testing, see Table 3, which can

help to overcome some of the obstacles that prevent women in developing countries so that they could also be tested for cervical cancer.

1.2.1. Pre-cancer tests

(WHO, 2021, CANCSA, 2016).

This is a test that is performed to test for cervical cancer by checking abnormality in cells that are located near or around the cervix.

a. HPV test - Where a small scrape inside or outside of the cervix is tested, where the presence of DNA or RNA of HPV is checked, which have the ability to cause pre-cancerous lesions, specifically HPV-16 and HPV-18.

b. Pap smear - Where cells are scraped outside or inside the cervix, removed and tested for any abnormality, such as pre-cancerous lesions.

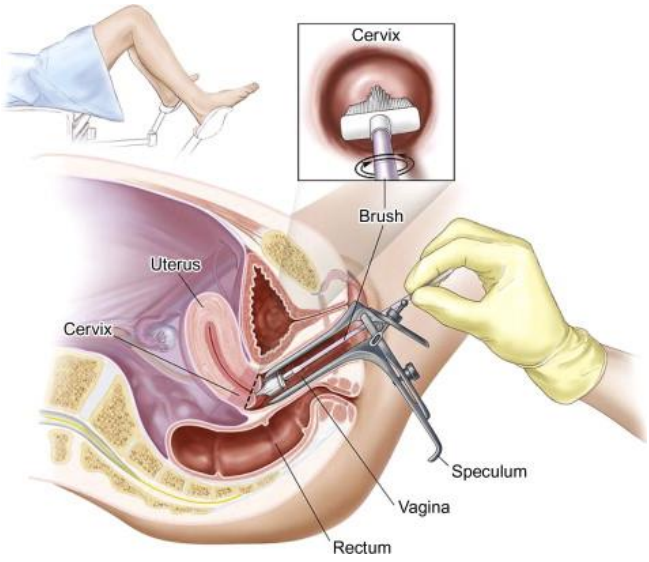

Figure 3**:** Cervical cytology sampling (papanicolaou test)
(Chevarie-Davis and Franco, 2013).

1.2.2. Tests after cervical cancer diagnosis

(WHO, 2021, Vordermark, 2016, Li et al., 2016b).

These are tests that are done after the cancer is confirmed. These tests help to determine the stage of the cervical cancer by looking into the size, location, and affected areas.

a. Radiology - This is an imaging test, where a picture of the inside of the body, where tumor is believed to be located is taken. This image is taken using ultrasound, X-rays or low levels of radiations, which are emitted from the site or emitted outside the body to the target area to image the inside of the body.
b. Endoscopy procedures - This is a medical procedure, where doctors place a tube-like instrument inside of the body, which helps to detect any abnormality within the body even to detect tumors.
c. Biopsy and cytology tests - The removal of samples of tissues within the human body in areas, where there is an abnormality, which will be viewed under a microscope by a pathologist

1.3. Cervical cancer treatment

The treatment of choice for cervical cancer depends on the tumor stage and the nodal status, as well as several clinical factors. Radical or fertility sparing surgery is reserved for cases with early-stage organ-confined disease. For the locally advanced or node-positive disease, external beam radiation therapy (RT) with concurrent cisplatin chemotherapy, followed by intrauterine brachytherapy is the treatment of choice (Khan et al., 2016, Duenas-Gonzalez et al., 2014). However, resistance to radiation is a common phenomenon and a major obstacle in cancer therapy. The 5-year overall survival rates for stages II, III and IVA, are still only 64 percentage, 40 percentage and 15 percentage, respectively. Especially in low-income countries, treatment is still not accessible to all (Khan et al., 2016, Olpin et al., 2018). Alternative targeting approaches are urgently warranted and should be evaluated in combination with other treatment strategies, such as radiation and chemotherapy.

1.3.1. Standard therapy

Cervical cancer can be successfully treated but treatment is dependent on the stage and location of the cancer, as defined by the International Federation of Gynecology and Obstetrics (FIGO) (NCI, 2021b, Gupta, 2019) see Table 3. In the early stages of cervical cancer, the most common therapy is surgery since the tumor is in a local region

of the cervix and has not spread to distance organs. For micro-invasive carcinoma (stage IA1), conization with adequate excision margins instead of simple hysterectomy is considered effective. For stage IA2, acceptable approaches include conization or simple hysterectomy with pelvic lymphadenectomy and radical hysterectomy. In the case of small volume macroscopic disease (IB1 and IIA1), radical hysterectomy is standard but radical trachelectomy plus lymphadenectomy can be used to preserve fertility (Duenas-Gonzalez et al., 2014). Adjuvant systemic treatment is not necessary for early stage cervical cancer unless a high-risk factor for recurrence was identified in the surgical specimen then adjuvant chemoradiation is usually suggested (Lapresa et al., 2015). For locally advanced cases (IB2-IVA), chemoradiation is the primary treatment. The benefit for adjuvant systemic chemotherapy and neoadjuvant chemoradiation for this patient group is still under study in Phase III trials (Gupta, 2019). In advanced stages or metastatic stages, chemotherapy with external beam radiation cisplatin or brachytherapy is the treatment of choice. For most and recurrent or persistent disease not amenable to curative treatment bevacizumab, which is a targeted therapy, is added and can increase progression-free survival (PFS) and also the overall survival (OS) (Selvaggi et al., 2006) .

Table 4**:** Cervical cancer treatment based on stages
(Duenas-Gonzalez et al., 2014).

Stage		**Treatment**
Early stage	Stage IA1	Surgery: conization or hysterectomy
	Stage IA2, IB, IIA	Chemo-radiation, hysterectomy
Intermediate stage	Stage IIB, III, IVA	Chemo-radiation and surgery before or after, hysterectomy, external beam radiation.
Advance stage (metastatic stage)	Stage IV and recurring cancer	Surgery, hysterectomy, Chemo-radiation, external beam radiation cisplatin brachytherapy cisplatin or carboplatin. Advanced new therapies.

1.3.2. Treatment strategies for metastasized cervical cancer

Metastasis occurs when cancer that developed from one region affects a distant region in the body. There are two different forms of cervical cancer metastasis which, are lymphatic metastasis, where cancer spreads through skin and lymph nodes and hematogenous metastasis, where cancer spreads through blood to distance organs, which are different from direct invasion, where the tumor grows into the tissue, where it originated (CANCSA, 2016). In the case of lymphatic metastasis, chemotherapy and radiotherapy are more effective as the lymph node (LN), where pelvic organs are affected can be a distance lymphatic or isolated lymphatic, which is recurring. In the cause of hematogenous metastasis, surgery is more suitable as the cancer affects organs such as the lungs, bones, liver, and brain but is more beneficial when combined with chemotherapy. For direct invasion metastasis also, treatment by chemotherapy is the best treatment strategy (Li et al., 2016b).

1.3.3. New therapies for cervical cancer

With the high chances of recurrent cancer or cancer radioresistance, the development of new therapies is urgently needed. New cancer therapy developments have the aim to inhibit the growth of cancer through targeted therapies, such as anti- angiogenic agents and tyrosine kinase inhibitors. Using targeted therapies, only cancer cells are affected and combined with radiation, better treatment responses have been noted in advanced stages. One of the major factors that is known to increase the chances of developing cervical cancer is HPV, this is based on how HPV disease has the ability to change the DNA and RNA (Marquina et al., 2018). It has been proven in recent studies that the use of both vaccine therapy and immunotherapy improves the chances of survival of patients with advanced or recurring cervical cancer (WHO, 2021, Health, 2017). The anti-angiogenic drug, avastin or better known as bevacizumab, blocks the vascular endothelial growth factor 2 (VEGF-2) to decrease the blood supply of the tumor and combined with chemotherapy, it can improve the survival rate of advanced stages (metastasis stages) or recurrent cervical cancer (Crafton and Salani, 2016, Marquina et al., 2018). Next to anti-angiogenic treatments and immunotherapy, also targeting DNA

repair using poly adenosine diphosphate-ribose polymerase (PARP) inhibitors gained attention (Lightfoot et al., 2020).

1.4. Problem statement

The increase in the rise of death due to cervical cancer in women has led to the increased awareness of cancer in women. Cervical cancer is the third most common cause of death of women in developing countries with around 570 000 cases of cervical cancer and 311 000 deaths recorded worldwide in 2018 (WHO, 2021). In South Africa, about 5743 new cause of cervical cancer are reported and with an annual death 3027 due to cancer, about 90 percentage of cases are HPV-related (Denny, 2010). This has led to the development of new techniques in treating, preventing and screening for cervical cancer in women (Shafabakhsh et al., 2019). Despite improvements, there are other factors that are still an issue. Cervical cancer has little symptoms, which can easily be ignored or misinterpreted, leading to people finding out about the cancer later when the cancer has reached stage three or four. There is no home testing that women can follow like breast cancer to test for cervix cancer, only a yearly checkup based on the screening recommendation by the Department Of Health of South Africa. This knowledge of testing is new to developing counties as this type of cancer is not well known as a disease that affects young people (Tapera et al., 2019).

The sudden emergence of death of woman in developing countries due to cervical cancer has resulted in the health organizations questioning the health status of young women by focusing on the medical schemes or practices that are followed by young women in developing countries. From their understanding, these young women are not given the right to medical care or treatments and there is still a lack of education on sexual health. It is well known that cancer can be successfully treated when it is detected in its early stages of development (Reiss and Saftig, 2009). There are two common ways to treat cancer, which are by surgery if the tumor is easily located and can be physically removed from the body or by radiation, where the cancer is exposed to certain levels of radiation, causing damage to the DNA structure of the tumor,

instigating it to shrink. However, the use of radiation to treat cancer has also lead to the development of radioresistance, where CSCs play an important role (Olivares-Urbano et al., 2020). In the case of cervical cancer, cervical cancer stem cells (CCSCs) play a role in the relapse after radiation treatment and tumor metastasis (Huang and Rofstad, 2017). Other factors that influence radioresistance are the TME and DNA repair mechanisms that take place upon DNA damage induction. Hence, there is an increased interest to find radiosensitizers that can improve the effectiveness of current cancer therapies.

The goal of a radiosensitizer is to increase cytotoxicity of ionizing radiation by causing the acceleration of DNA damage and the production of free radicals, which increase the killing of cancer cells. The inhibitor allows an increase in radiation absorption in selective tissue cells and as a result, causing the cancer cells to experience more radiation absorption compared to healthy cells that are located within the same region. The use of radio-sensitizers to increase cancer cell death while using lower levels of radiation at sensitive organs can also prevent the development of secondary cancer due to RT. However, there is still a need to find effective radiosensitizers for the treatment of cervical cancer. No targeted drug has been developed specifically for cervical cancer but antiangiogenic therapy, such as bevacizumab has shown promise Duenas-Gonzalez et al (2014). The ADAM10 inhibitor that was used in this experiment was selected due to the role of ADAM10 in the RR activation of Notch and the specific EGFR ligands (Mullooly et al., 2016). In addition, ADAM10 has shown to be associated with cancer formation and progression. ADAM10 and ADAM17 inhibitors can have an anti-cancer ability by blocking the release of ligands that normally activate cell proliferation, cell survival and protein synthesis (Duffy et al., 2011).

1.5. Aims and objectives

1.5.1. Aim

The aim was to determine the effectiveness of an ADAM10 inhibitor as a radiosensitizer for the treatment of cervical cancer. We selected the commercially available peptide

based ADAM10 inhibitor, GI254023X, as a potential radiosensitizer in this study. Inhibition of ADAM10, a member of the (ADAM) family, has been considered as a promising novel targeted cancer strategy (Wetzel et al., 2017). In addition, due to its role in the Notch signaling pathway, blocking ADAM10 could enhance the effectiveness of RT. ADAM10 influences the TME due to its effect on survival pathways that can cause tumor proliferation, angiogenesis and affect the immune response (Waller and Pruschy, 2021).

1.5.2. Objectives

In this dissertation the objective was to answer these questions:

- To determine the effect of the ADAM10 inhibitor on the cell survival and proliferation activity of the cervical cell with and without combined photon irradiation.
- To optimize the apoptosis assay for Hela cells and compare the amount of apoptosis induced by the ADAM10 inhibitor with and without combined photon irradiation.
- To optimize the migration assay using inserts and the invasion assay and determine the inhibitory effect of the ADAM10 inhibitor on the migration and invasion of the cervical cancer cells with and without combined photon irradiation.

Chapter 2: Literature review

2.1. Radiotherapy and radio-sensitization

2.1.1. What is radiotherapy?

Radiation is a form of energy that has a high frequency and short wavelength, which can penetrate through various materials. There are two different types of radiation, known as ionizing and non-ionizing radiation, which are grouped based on their ability to break the atomic structure of a material (Ryan, 2012). Non-ionizing radiation, such as heat, light, radio wave and microwave can transfer energy onto an atom, but the energy does not have the ability to break the bonds of the molecule or remove a particle in the atom. Ionizing radiation, such as gamma ray, X-ray and cosmic ray are high energy radiations, which have that ability to break the bonds of material and can cause removal of particles within an atom (Ryan, 2012, Ojovan et al., 2019).

Radiation is the general technique that is used to treat cancer through RT. Treatment of cervical cancer may variously depend on the stage and area in which the cancer is located as seen in Table 4. The most performed radiation treatment is external beam radiation therapy (EBRT) with X-rays or gamma radiation or the use of brachytherapy and concomitant chemotherapy. EBRT can use either X-ray or gamma radiation to treat cancer by damaging the tumor cells causing them to reduce the size of the tumor. The use of advanced radiotherapy techniques based on EBRT through the use of intensity-modulated radiotherapy (IMRT) is known to be beneficial to patients with cervical cancer by reducing gastrointestinal toxicity and potentiating dose escalation due to radiation exposure. By dividing the radiation dose into intervals, which are based on the location of the cancer, size of the cancer, risk of treatment due to organs located near the cancer and the desired targeted outcome of the treatment (Jadon et al., 2014, Vordermark, 2016).

Brachytherapy is an internal radiation treatment to help treat cancer by giving high dose of radiation to the tumor and less to healthy cells or organs that are located near the tumor, which is achieved by using magnetic resonance imaging (MRI) or computed

tomography (CT), where a radioactive substance is placed inside the body near the tumor (Banerjee and Kamrava, 2014). This treatment mostly uses short half-life radioactive source such as iodine-125, palladium-103 and iridium-192 (L'Annunziata, 2016, Kirisits et al., 2006).

Chemotherapy is mostly a neoadjuvant treatment instead of an adjuvant treatment that is done after other treatments. During chemotherapy, a drug is injected into the vein or given orally that circulates around the body or it can stay local. Unlike brachytherapy, chemotherapy uses chemicals that attack fast growing cells in the body. A chemo drug such as gemcitabine is generally used to treat solid tumors and in ovaries cancer, but all chemo drugs cannot tell the difference between cancer and healthy cells (Selvaggi et al., 2006, Lapresa et al., 2015). The use of chemotherapy has improved the chances of survival of cancer cells but there are still other factors such as the high risk to patient such as toxic side effects and even the development of resistance can also occur. This is why when treating cancer other treatment strategies are taken into consideration such as targeted therapy.

In certain cervical advanced cancer cases, the use of a combined treatment is taken into consideration (Cree et al., 2018). By using combined therapy, EBRT focuses on the pelvic lymph nodes, parametric and primary cancers while brachytherapy can improve the cancer control and survival rate of the patient. With additional chemotherapy, tumors can become more sensitive to radiation with a subsequent increase in tumor cell death and a reduced radiation dose required to successfully treat the cancer (Banerjee and Kamrava, 2014).

2.1.2. What is a radiosensitizer?

Radiosensitizers are substances that can enhance the killing of tumor cells through the acceleration of DNA damage and the formation of free radicals when used alongside RT (Koch et al., 2010). These substances are believed to be very effective is treating cancer as radiosensitizers have little effect on normal cells, reducing the damage to normal cells that are located near the tumor cells. For a compound or a drug to be

called a radiosensitizers, it must have a good therapeutic index (TI), which can allow us to determine how much effect the substances had on the tumor cells comparing it to the damage that occurred in normal cells (Marcu, 2013).

Gong et al (2021) has classified radiosensitizers into three different categories: small molecules, macromolecules and nanomaterials. For a substance to be considered a radiosensitizer, it needs to have one of the following actions: (i) inhibit radiation-induced repair of DNA damage, (ii) disturb the cell cycle and organelle functions to help improve cytotoxicity and (iii) inhibit the expression of genes that induce radiation resistance or promote the expression of radiation sensitive genes (Gong et al., 2021).

2.1.3. Cervical cancer radioresistance

Cancer growth and development is affected by many factors, which lead to the inability for radiation therapy to reach its maximal potential. Considering how the body cannot distinguish between normal cells and cancer cells when the body is under attack, radiation can induce genotypic or phenotypic changes that can prevent cell death or change the tumor microenvironment (TME) that increases tumor survival (Kalyanaraman, 2017). Factors such as an enhanced DNA damage response and repair, presence of cancer stem cells (CSCs) within the tumor, deregulated signaling pathways and TME can cause the development of radioresistant cancer cells that survive after radiation exposure (Gray et al., 2019).

The ability for cells to repair themselves is a crucial role that is played by the genes called the DNA damage response (DDR) and repair genes that takes place during the cell cycle arrest induced by checkpoints during the growth phase 1 (G1), synthesis phase (S) and the mitosis phase (M) of the cell cycle (Lamberti et al., 2020). In the case of CSCs, when put under pressure due to a change in the environment, this can lead to cells undergoing differentiation, causing a change in the phenotype function that can lead to cells becoming radioresistant (Li et al., 2016a). Heterogeneous tumors are made up of both CSCs and non-CSCs. The CSCs only make up a small subpopulation of cells that make up the tumor, which can lead to radioresistance because they can self-renew

and differentiate into heterogeneous cancer cell lineages that later will make up the whole tumor (Olivares-Urbano et al., 2020).

Cancer cell growth and progression is also impacted by the environment in which the cancer cells are growing, consisting of the immune response, blood vessels and inflammatory response. The latter form a complex system that supports the growth of cancer cells by providing nutrients and oxygen to ensure the cancer progresses and spreads, thus implying that the microenvironment also needs to be desirable for tumor to grow (Suwa et al., 2021).

Radiation is known to have the ability to cause the induction of cytotoxicity but there are multiple pro-survival signaling pathways that can also be activated, which can lead to the suppression of apoptosis and prevention of cell cycle arrest and development of radioresistant cancer (Hein et al., 2014). For example, the Hedgehog signaling pathway plays a role in the invasion, metastasis, drug resistance and growth of cervical cancer (Liu and Wang, 2019). The PI3K/Akt (phosphoinositide 3-kinases) signaling pathway can also cause radioresistance by causing the up-regulation of the interleukin-11 (IL-11), affecting cell proliferation, migration and controlling the metabolism of cell (Sun et al., 2021). The Ras-ERK/MAPK-ERK (mitogen-activated protein kinases-extracellular signaling-regulated) signaling pathway is an extracellular signaling pathway that regulates kinases, controlling signals from the plasma membrane to the nucleus (Bugaj et al., 2018, Gong et al., 2021). The Ras-ERK and the PI3K/Akt signaling pathways have the ability to prevent apoptosis, resulting in the survival of damaged cells(Sever and Brugge, 2015, Bugaj et al., 2018, Su et al., 2012). In this dissertation, we looked at the possible radiosensitizing effect of an ADAM10 inhibitor to improve the treatment of cervical cancer.

2.2. ADAM10 inhibitor as a radiosensitizer for cervical cancer

2.2.1. What is ADAM?

The disintegrin and metalloproteinase (ADAMs) are a group of transmembrane multidomain proteins that have biochemical mechanisms that regulate a variety of

activities in a cell such as proteolysis, cell adhesion and cell migration (Smith Jr et al., 2020, Mullooly et al., 2016). ADAMs are enzymes that have the ability to breakdown proteins into smaller polypeptides. There are different types of metalloproteinases, which have been discovered in different species while there are 22 members that are currently in the family of human ADAM metalloproteinases. The ADAM family is a subgroup of metzincin proteins, which are similar to the matrix metalloproteinases (MMPs) and are a zinc protease superfamily as the zinc-binding consensus motif is used as the activity site of the inhibitor (Waller and Pruschy, 2021, Mullooly et al., 2016). The activity of MMPs and ADAMs are modulated by tissue inhibitors of metalloproteinases (TIMPs), which are small endogenous protein inhibitors. There are four types of TIMPs (TIMP1-4) which all have their own selective MMP-binding ridges (Duan et al., 2015).

ADAMs have the biological ability to cause proteolysis of substrates that are ectodomains of type I and type II transmembrane proteins and include precursor forms of growth factors, cytokines and adhesion proteins (Wetzel et al., 2017, Mullooly et al., 2016). ADAM proteins have the ability to regulate intramembrane proteolysis with the site of binding motif HEXXHXXGXXH and shedding of substrates that target cancer progression and inflammation pathways, such as the Notch, E-cadherin, epidermal growth factor (EGF), ErbB3 and inflammatory cytokines (see Figure 4) (Crawford et al., 2009). By disrupting the cleavage of these substrates and their downstream pathways, we may slow down the growth and formation of cancer cells and preventing them from spreading within the organism's body (Wetzel et al., 2017). Based on the biological role of ADAMs, there is evidence that shows that ADAM8, ADAM10, ADAM17 and ADAM28 have protease activity in cancer formation and progression (Mullooly et al., 2016).

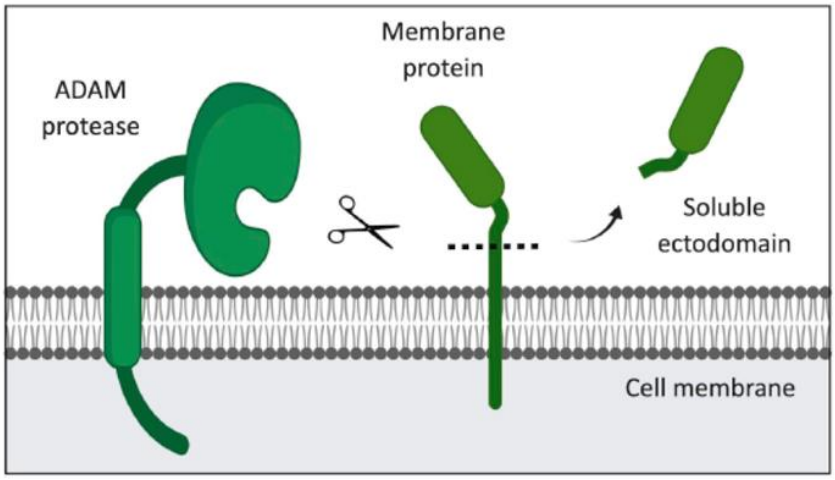

Figure 4**:** Sheddase activity of ADAMs
(Saad et al., 2019).

2.2.2. ADAM10 as a target for cancer therapy and radiosensitization

When cancer cells are irradiated, next to direct cell killing, there are intra and intercellular actions that take place in the TME that stimulate cancer radioresistance (Waller and Pruschy, 2021). Zinc-MMPs play a role in the irradiation induced secretion of pro-survival factors that affect radioresistance. These factors can cause signals that can favor cancer death or proliferation, survival, and even the ability to adapt hypoxia (Reczek and Chandel, 2017). The secretion of pro-survival factors, growth factors, chemokines and cytokines and reactive oxygen species (ROS) within the TME upon irradiation, can on their turn, activate MMPs. Hence, members of the ADAM family co-determine the RR, see Figure 5 (Waller and Pruschy, 2021). .

In this study, we selected ADAM10 as an anti-cancer target (Rong et al., 2017, Parkin and Harris, 2009, Rocks et al., 2008). ADAM10 and ADAM17 both have an N-terminal signal sequence and an adjacent prodomain, which is followed by a metalloproteinase, cysteine-rich domain and disintegrin (Seegar et al., 2017). Inhibition of ADAM10 has been considered as a promising targeted cancer strategy, however, the fact that ADAM10 sheds a number of substrates, such as (EGF), N-cadherin cleavage (neuroligin-3) through the PI3K-mTOR pathway and Notch1, ADAM10 could be a

potential radiosensitizer. Notch1 plays a key role in tumor initiation, progression, apoptosis, cell survival and treatment response (Liu et al., 2015).

ADAMs have the ability to stimulate the formation and metastasis of cancer by shedding molecules that contribute to proliferation, differentiation, adhesion and migration, such as the Notch, E-cadherin, CD44 and L1. Hence, blocking ADAM10 could help in treating cancer. The dissertation by Wagiet (2016) proved that ADAM10 activity is present in cervical cancer cells with most activity present in the mesenchymal cells (Moss et al., 2008, Wagiet, 2016). To understand how the inhibition of ADAM10 can help in cancer treatment, we looked into the TME, where the activity of MMPs can cause cancer progression. If there is a higher number or activity of MMPs, there is a higher chance of cancer cell invasion into surrounding tissue and blood vessels, which can also be induced by radiation (Waller and Pruschy, 2021). Out of the 22 human ADAM families, only half of them have the MMP like protease: ADAM9, ADAM10, ADAM12, ADAM17, ADAM19, ADAM28 and ADAM33 (Duffy et al., 2011). Other cancer studies, where ADAM10 was investigated, such as pancreatic, breast, melanoma and bladder cancer cells, it was shown that the biological activity of ADAM10 can be cell type specific due to the substrate that is being taken into consideration (Mullooly et al., 2016). This can be seen in a study done by Mullooly et al (2016) that showed that when ADAM10 is targeted in breast cancer, there is a decrease in cell invasion and cell migration but little effect on cell proliferation. In contrast, when pancreatic cancer cells are taken into consideration, there is also a decrease in cell migration and cell invasion but no effect on cell proliferation (Duffy et al., 2011).

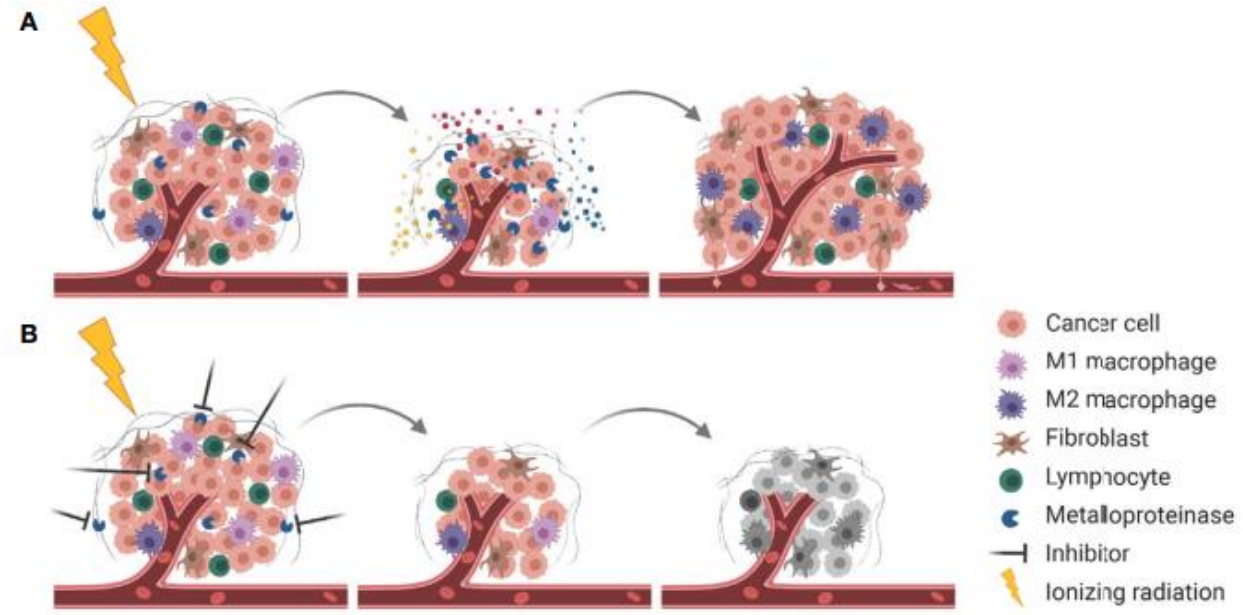

Figure 5**:** Radiation induces tumor immune repaired due to radiation.
(Mullooly et al., 2016).
Part (A) shows that after irradiation, MMPs play a role in the release of pro-surviving factors in the TME, inducing tumor cell proliferation, a pro-tumorigenic immune response and enhance tumor angiogenesis. Part (B) shows how the use of combined therapy prevents pro-survival signals resulting in tumor death.

2.2.3. Role of the Notch pathway in radiation resistance

Notchs are known as short range cell to cell signaling proteins that act as receptors that help in the development of cells and in adult cells they have the ability to self-renew, cause differentiation and proliferation (Yahyanejad et al., 2016). There are 4 Notch receptors (Notch1-4) and 5 ligands (delta-like1-4) that work together to send signals from one cell to another, which can cause proteolysis cleavages that cause the release of Notch intercellular domain (NICD). Notch 1 is a ligand of ADAM 10. The role of Notch signaling in human cervical cancer and radiation resistance has been reviewed, (see (Yahyanejad et al., 2016, Maliekal et al., 2008). Notch plays a role in radiation resistance through intrinsic and extrinsic mechanisms with the intrinsic causing radiation resistance by pathways that play a role in survival factors, DNA repair and even cell death through apoptosis, while the extrinsic factors affect radiosensitivity through extracellular matrix molecules, hypoxia cytokines and angiogenesis (Yahyanejad et al.,

2016). Cancer hypoxia is the region within a tumor, where the level of oxygen tension is lower than 10 mmHg and because of this, the tumor may become radioresistant since oxygen is needed for the cytotoxic effect of radiotherapy. Angiogenesis is the process, where the tumor is triggered by chemical signals, causing the formation of vascular networks that provide nutrients and oxygen to the tumor through the formation of blood vessels (Qin et al., 2014).

Intrinsically, Notch has a direct role in the DDR. Ataxia-telangiectasia mutated (ATM) is activated specifically upon double strand (ds) DNA breaks induced by ionizing radiation. Notch1 directly binds to ATM, thereby inactivating its kinase activity. Blocking Notch using a γ-secretase inhibitor (GSI) in the presence of DNA damage, leads to increased radiation sensitivity in an ATM-dependent manner (Yu et al., 2012, Yahyanejad et al., 2016). The link between hypoxia and Notch signaling has also been described in various studies (Purow, 2009, Lee et al., 2010, Qin et al., 2014, Reczek and Chandel, 2017). Data suggest that Notch signaling may increase the survival of hypoxic cells and thereby influencing the response to RT (Yahyanejad et al., 2016). Finally, Notch inhibitors can inhibit stromal and cancer cell synthesis of some inflammatory cytokines, including tumor necrosis factor (TNF), IL-6 and IL-8 in the TME. These cytokines are associated with radioresistance, metastasis, proliferation and the maintenance of CSCs (Yu et al., 2012). Hence, combining Notch therapeutics with irradiation may lead to synergistic improvements (Gersey et al., 2019, Yahyanejad et al., 2016). Another advantage of radiosensitizers is the possibility to reduce the radiation dose to the patient, limiting the dose to neighboring healthy tissues and possible related side effects(Koch et al., 2010, Purow, 2009). A schematic of the Notch pathway is given in Figure 6.

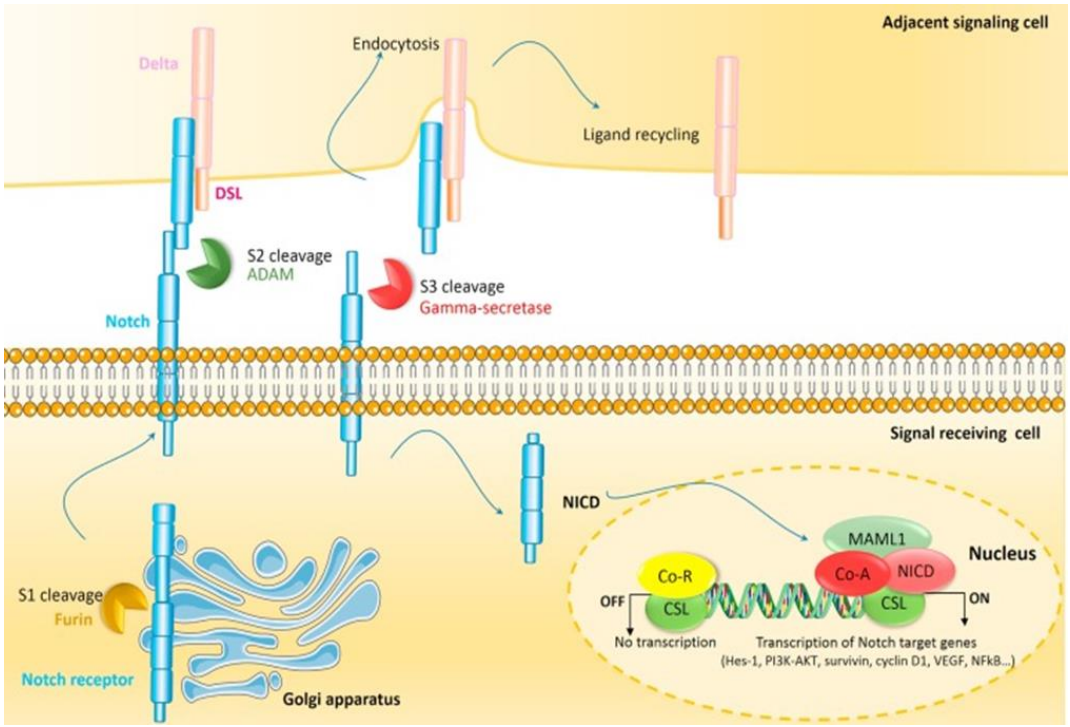

Figure 6**:** Notch signaling pathway
(Majidinia et al., 2018).

2.2.4. The ADAM10 inhibitor GI254023X

Targeted compounds, such as radiosensitizers and inhibitors, have the aim to ameliorate the treatment response of cancer while reducing damage to health cells that are located near the tumor cells. In this dissertation we studied the radio-sensitizing effects of the commercial ADAM10 inhibitor GI254023X (Waller and Pruschy, 2021). This small molecule inhibitor is a N-formyl hydroxylamine-based inhibitor, which has inhibitory potential by chelating Zn^{2+} of the active sites and possesses almost a 100-fold sensitivity for ADAM10 versus other ADAMs (Bazzoni and Bentivegna, 2019). The bulky aromatic group of GI2540230X is believed to have the ability to cause the interaction with the S1exosite, causing them to be metzincin selective inhibitors (Liu et al., 2015).

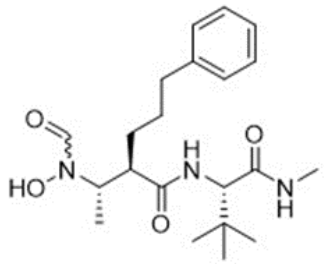

Figure 7**:** Chemical structure of GI254023X
(Waller and Pruschy, 2021).

Studies have shown that the intercelluar and extercellualr activity of the MMPs affect the function of cells, where these proteins are involved in cell adhesion and receptor signaling, which can initiate proteolysis of cells (Wetzel et al., 2017). There are different types of inhibitors of MMPs, which have a low molecular weight or monoclonal antibodies (Mullooly et al., 2016). Low molecular weight hydroxamate-based inhibitors are said to have a cataytic activity using their zinc chelating active site. There are four generations of MMP inhibitors, with each generation improvements was made from the previous generation. The development of the first generation of MMP inhibitors with a hydroxamated zinc binding group had strong side effects such as inflammation, peripheral edema pain on the musculoskeletal system and nausea, causing them to fail clinical trials and also because they are not very selective (Wetzel et al., 2017, Li et al., 2020). The second generation ones are non-hydroxamated based inhibitors, which have a weak affinity for the catalytic Zn^{2+} (Li et al., 2020). The third generation are non-zinc binding inhibitors while the fourth generation includes allosteric and exosite inhibitors (Li et al., 2020). GI254023X is a hydroxamate inhibitor with almost a 100-fold sensitivity for ADAM10 than other ADAMs - making it a more selective inhibitor of ADAM10 (Seifert et al., 2020).

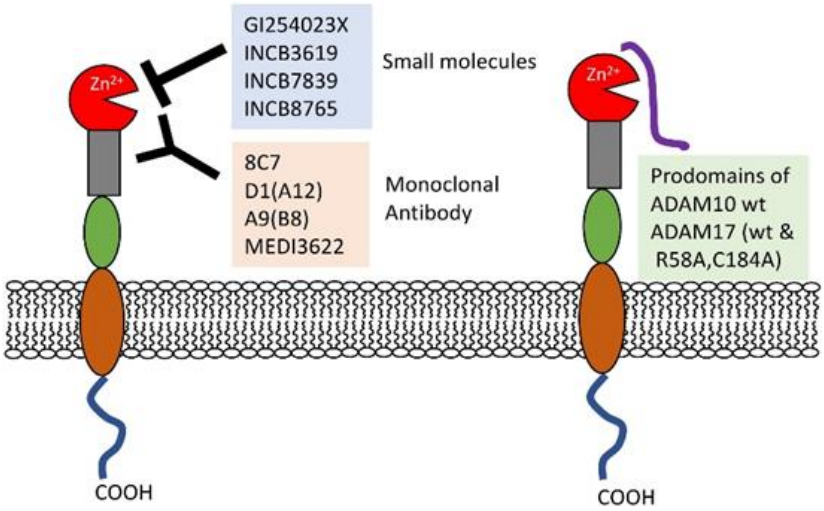

Figure 8**:** Overview of ADAM10 inhibitors, both small molecules including the GI drug and monoclonal antibodies
(Kato et al., 2018).

Chapter 3: Methodology

All experiments were performed at iThemba LABs under the supervision of Dr. Julie Bolcaen, Dr. Shankari Nair, and PhD student / lab technician Xanthene Muller. All equipment needed was available at iThemba LABS:

- Co-60 source to perform gamma irradiation
- Sterile cell culturing facility
- Flow cytometry (BD Accuri C6 flow cytometer)
- Live cell imaging system (Lonza Cytosmart)
- Specialized equipment and radiobiology techniques

3.1. Cervical cancer cell lines

In this study, we used 2 different human cervical cancer cell lines (Hela and C33A) to test the effectiveness of the ADAM10 inhibitor (GI254023X) as an anti-cancer drug and radiosensitizer. The characteristics of both cell lines are listed in Table 5.

Table 5**:** Characteristics of the cervical cancer cell lines (Collection, 2020).

Characteristics	**Hela**	**C33A**
Name	Hela (ATCC® CCL-2™)	C-33a (ATCC®HTB-31™)
Organism	Homo sapiens	Homo sapiens
Tissue	Uterus, Cervix	Uterus, Cervix
Cell type	Epithelial	Epithelial
Disease	Adenocarcinoma	Carcinoma
Morphology	Epithelial	Epithelial
Culture properties	Adherent	Adherent
HPV status	+ HPV18	Negative
p53 status	Wild type	Mutated

3.2. Cell culturing

All cell culturing was performed in the biosafety cabinet (Lab Tech, Class 2 BSC), where the surface was wiped with 70 percentage ethanol and any material or substances that enter the biosafety cabinet were wiped with 70 percentage ethanol to maintain a sterile environment.

3.2.1. Materials for cell culturing

- Cryovials containing frozen cells (stored at -80°C)
- Complete growth medium, pre-warmed to a temperature of 37°C
- Disposable, sterile centrifuge tubes
- Water bath set at a temperature of 37°C
- 70 percentage ethanol
- Tissue-culture treated flasks (NEST, South Africa)
- Waste beaker
- Sterile PBS, pre-warmed to a temperature of 37°C
- Trypsin, pre-warmed to a temperature of 37°C
- Incubator (5 percentage CO2, 37°C)

3.2.2. Cell growth media

The cell culture media was based on the growth requirements of the cervical cancer cells. For culturing, the Hela cancer cells, complete RPMI consisting of RPMI media (Lonza, Belgium) with 10 percentage FBS (Gibco, South America) and 1 percentage of penicillin / streptomycin (Lonza, Germany) was used, while for culturing the C33A cervical cancer cells, complete EMEM was used that consisted of EMEM media (Lonza, Belgium) with 20 percentage FBS and 1 percentage penicillin / streptomycin. The complete media was warmed up to 37℃ using the warm water bath before use.

3.2.3. Culturing cervical cancer cells

a. Starting up cell cultures

The cervical cancer cells were stored at -80°C in FBS containing 10 percentage dimethyl sulfoxide (DMSO) (Calbiochem, San Diego). To start up cell cultures, the cryovial was thawed in a 37°C warm water bath (< 1 minute). Once thawed the cells were quickly transferred into a 15 mL centrifuge tube and 6 mL of pre-warmed complete media was slowly added. The tube was centrifuged to form a pellet and the supernatant (containing the toxic DMSO) was removed. The pellet was resuspended in 4 mL of pre-warmed complete media and transferred into a T25 culture flask. The culture flask was placed in the incubator (37°C, 5 percentage CO_2) (Thermo Scientific, Direct heat CO_2 Incubator) and attachment was closely followed up.

b. Maintenance of the cell cultures

Depending on the doubling time of the Hela and C33A cell line, the culture flasks reached confluency within a few days. To continue culturing at that point, the cells needed to be loosened first and reseeded into new flasks (called splitting the flasks). First, all media was removed from the cell culture flask and subsequently the flask was washed with 1 mL of sterile PBS (Gibco, UK). After, 1 mL of trypsin 2X (Lonza, UK) was added and the flask was transferred to the incubator for 1-3 minutes. Loosening of the cells was closely followed up under the microscope (ZEISS, Primo vert). The bottom of the flask was gently tapped. Once all cells were detached from the surface, 6 mL of the pre-warmed respected complete media was added and transferred into a 15 mL centrifuge tube and centrifuged (Jouan, Thermo Scientific) during 5 minutes at 900 rpm. Supernatant was removed and the pellet was resuspended in 4 mL of pre-warmed complete media and divided in multiple flasks depending on the split ratio or experiment to be performed.

3.3. Treatment conditions

This study included four different treatment conditions to be able to define anti-cancer and radiosensitizing effects of the GI drug as a monotherapy or combined with RT:

A. Controls
B. Radiotherapy
C. GI254023X + radiotherapy
D. GI254023X

3.3.1. GI254023X

To prepare 1 mM of stock solution of GI254023X (Sigma, USA), 1 mg of GI254023X was diluted into 2600 µL of RPMI. The concentration of GI254023X for Hela and C33A was determined using the MTT assay, where the IC_{50} was the concentration that was going to be added to the cells in the GI254023X treatment arms.

3.3.2. Radiation treatment

The radiation source used in the experiments is the ^{60}Co source located at the radiobiology lab of iThemba LABS. The radiation exposure time was calculated based on the dose rate of the source at the time of irradiation. The T25 flasks were placed between 5 mm thick perspex plates to ensure dose build-up and a 50 mm backscatter plate with a dose rate of 0.468 Gy/min for a 30 x 30 cm^2 field size at 75 cm source to surface distance (SSD).

Figure 9**:** ^{60}Co gamma source located at the Radiation Biophysics division of iThemba LABS

3.4. Assays

3.4.1. Colony survival assay (CSA)

After culturing the adherent cervical cancer cells lines (Hela and C33A) in T25 cell culture flasks, the cells were washed with sterile PBS, trypsinized and centrifuged. Using a hemocytometer, the total number of cells per 1 mL was determined from which, through serial dilution with complete media (100 percentage RPMI, 10 percentage FBS and 1 percentage antibiotics for Hela or 100 percentage EMEM, 20 percentage FBS, 1 percentage antibiotics for C33A), 5 samples of 100 000, 5000, 2500, 500 and 100 cells per 1 mL in 5 different sample tubes were prepared. Petri-dishes were labelled with 8, 6, 4, 2 and 0 Gy. 2 mL of complete media and 1 mL of 5000, 2500, 500 and 100 cells per 1 ml were added respectively in the labeled petri-dishes except for 2 Gy, where 0.5 mL containing 500 cells per mL was added. The petri-dishes were transferred into the incubator and irradiated 24 hrs later. This experiment was repeated in six different petri-dishes.

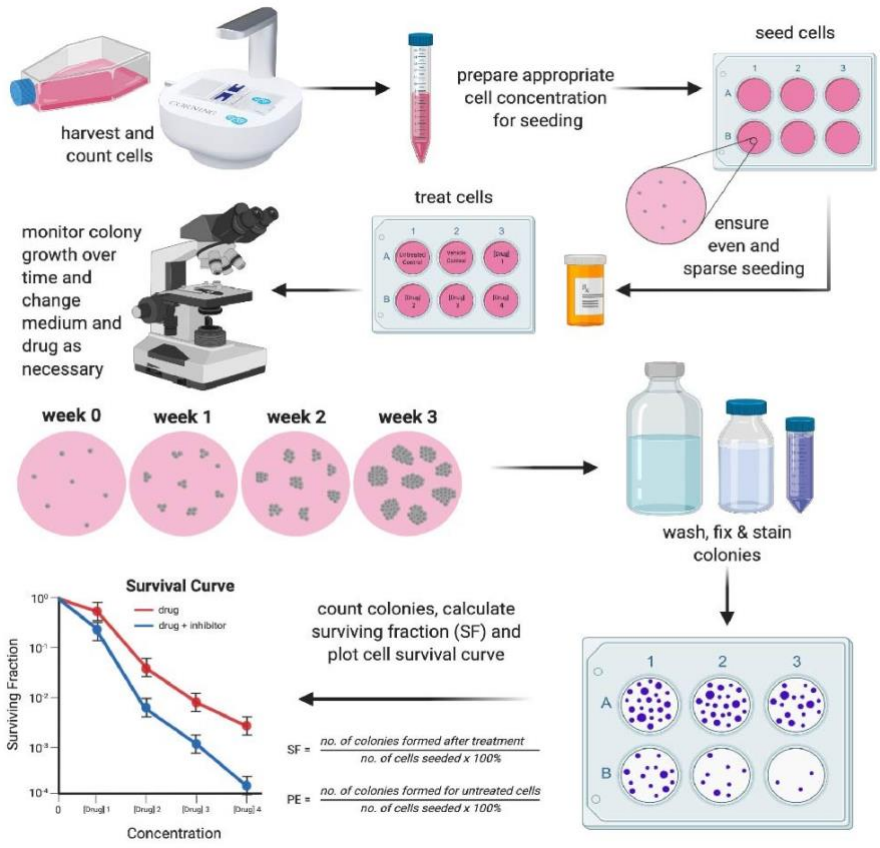

Figure 10**:** Schematic representation of a tradition clonogenic assay setup (Bleloch, 2020)

3.4.2. Optimization of the CSA

The applied dilution route to reach the desired cell count range for plating was:

$$100\,000 \xrightarrow{\div 20} 5000 \xrightarrow{\div 2} 2500 \xrightarrow{\div 5} 500 \xrightarrow{\div 5} 100$$

In one T25 cell culture flask, the total number of cells was 165 000 per 1 mL from which for the dose of 0 Gy, 206 cells were plated, for the dose of 2 Gy, 412 cells were plated, for the dose of 4 Gy, 825 cells were plated, for the dose of 6Gy, 4125 cells were plated and finally, for the maximum dose of 8 Gy, 8250 cells were plated, which was achieved through serial dilution in cRPMI as described here:

From cells from the cell culture flaks, 0.5 ml was dissolved in 9.5 mL of cRPMI to make 8250 cells per 1 mL

$$C_1V_1=C_2V_2$$

$$C_2 = \frac{C_1V_1}{V_2}$$

$$C_2 = \frac{(165000)(0.5mL)}{10mL}$$

$$\therefore C_2 = 8250\ cells \text{ per 1mL}$$

From which 1 mL was plated in 8 Gy labeled petri-dishes and 2 mL of cRPMI was added. From the dilution of 8250 cells per 1mL, we made 4125 cells per 1 mL by dissolving 3 mL in 5 mL of cRPMI:

$$C_1V_1=C_2V_2$$

$$C_2 = \frac{C_1V_1}{V_2}$$

$$C_2 = \frac{(8250)(3mL)}{6mL}$$

$$\therefore C_2 = 4125\ cells \text{ per 1 mL}$$

From which, 1 mL was plated in 6 Gy labeled petri-dishes and 2 mL of cRPMI was added.

From the dilution of 4125 cells per 1 mL, we made 825 cells per 1 mL by dissolving 2 mL in 8 mL of cRPMI:

$$C_1V_1=C_2V_2$$

$$C_2 = \frac{C_1V_1}{V_2}$$

$$C_2 = \frac{(4125)(2mL)}{10mL}$$

$$\therefore C_2 = 825\ cells \text{ per 1mL}$$

From which, 1 mL was plated in 4 Gy labeled petri-dishes and 2 mL of cRPMI was added.

From the dilution of 825 cells per 1 mL, we made 412 cells per 1 mL by dissolving 3 mL in 4 mL of cRPMI:

$$C_1V_1=C_2V_2$$

$$C_2 = \frac{C_1 V_1}{V_2}$$

$$C_2 = \frac{(825)(3mL)}{6mL}$$

$$\therefore C_2 = 412\ cells \text{ per 1mL}$$

From which, 1 mL is plated in 2 Gy labeled petri-dishes and 2 mL of cRPMI was added.

From the dilution of 825 cells per 1 mL, we made 206 cells per 1 mL by dissolving 0.5 mL in 2 mL of cRPMI directly into the petri-dishes:

$$C_1V_1=C_2V_2$$

$$C_2 = \frac{C_1 V_1}{V_2}$$

$$C_2 = \frac{(825)(0.5mL)}{2mL}$$

$$\therefore C_2 = 206\ cells \text{ per 1mL}$$

This dilution route was done for every preparation for CSA, where the total number of cells was determined within the cell culture flask for both the Hela and C33A cervical cancer cells.

3.4.3. Migration – wound healing assay

Migration assay, was also known as wound healing assay Kahl (2020) but throughout this dissertation we referred to it as the migration assay. To create a wound we used the 2 well Ibidi culture inserts (Ibidi, Germany), see Figure 11. After culturing the Hela cervical cancer cells in T25 cell culture flasks, the cells were washed with sterile PBS, trypsinized and centrifuged. The total amount of cells was counted using a hemocytometer. The ideal number of Hela cells to plate in the Ibidi migrations wells was first determined. The insert was first placed in a sterile 300 mm micro-dish. A total number of 100 000 cells seeded per chamber of the insert was ideal to reach a 100 percentage confluent monolayer inside the inserts within 24 hrs.

Through dilution with media, 200 000 cells were transferred into a 15 mL centrifuge tube, centrifuged during 5 min at 2000 rpm and supernatant was removed. The pellet

was resuspended in 140 µL of complete media of which 70 µL was transferred into each chamber of the Ibidi insert and the micro-dish was then placed in the incubator (5 percentage CO2, 37°C). 24 hrs later, the Ibidi insert was removed and cells were washed with 1 mL of complete media and 2 mL of complete media was added in case of a control condition or irradiation only (2 Gy) conditions. For the combined treatment conditions (GI and irradiation), 70 µL of GI working solution (20.3 µL in 1 mL complete media) was added to the chamber 2 hrs before irradiation. After irradiation, 40.6 µL of GI was added in 2 mL complete media for another 24 hrs. For the GI only conditions, the cells were also exposed to GI during 26 hrs.

After removing the Ibidi insert, the wound was placed in the field of view of the Lonza Cytosmart and closure was followed up (snapshots every 15 min) while the micro-dish was placed in the incubator.

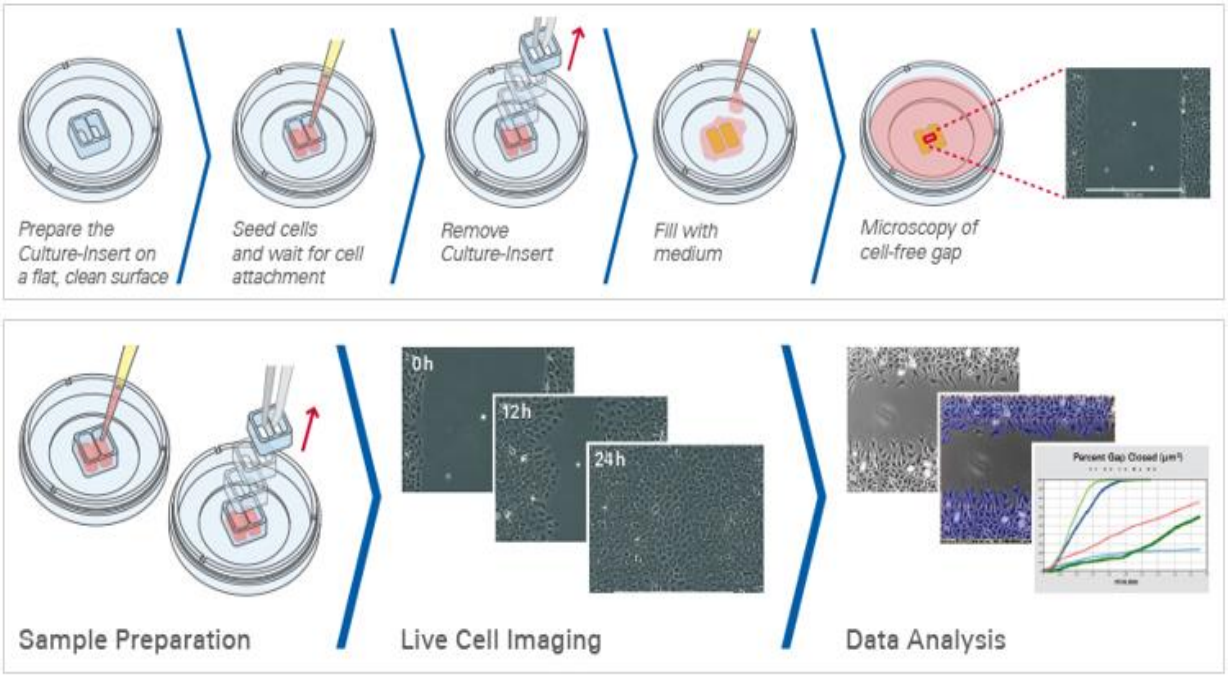

Figure 11**:** Experimental workflow for a wound healing assay using the 2 well Ibidi culture-insert
(Kahl, 2020, Juanes et al., 2020).

3.4.4. Optimization of the migration assay for Hela cervical cancer cells

Different amount of Hela cells (70 000, 100 000 and 300 000) were plated in the well chambers of the Ibidi migration wells to optimize the ideal cell count to reach full confluence within 24 hrs, (see Figure 12). To plate the desired number of cells, the following method was applied: For plating 300 000 cells per well in the 2 well Ibidi inserts, the total number of cells in a T75 cell culture flask was calculated (e.g. 3 550 000 cells in 5 mL). 600 000 cells were pipetted using the following calculation:

$$C_1V_1=C_2V_2$$

$$V_2 = \frac{C_1V_1}{C_2}$$

$$V_2 = \frac{(5000)(600000)}{3550000}$$

$$\therefore V_2 = 845\ \mu L$$

Hence, 845 µL contains 600 000 cells, which were centrifuged and re-suspended in 140 µL of cRPMI and 70 µL was seeded in each chamber of the Ibidi insert well and incubated for 24 hrs. Seeding 100 000 cells per well seemed to be ideal to reach a confluent cell layer in the chamber to obtain a free cell gap upon removal of the insert after 24 hrs.

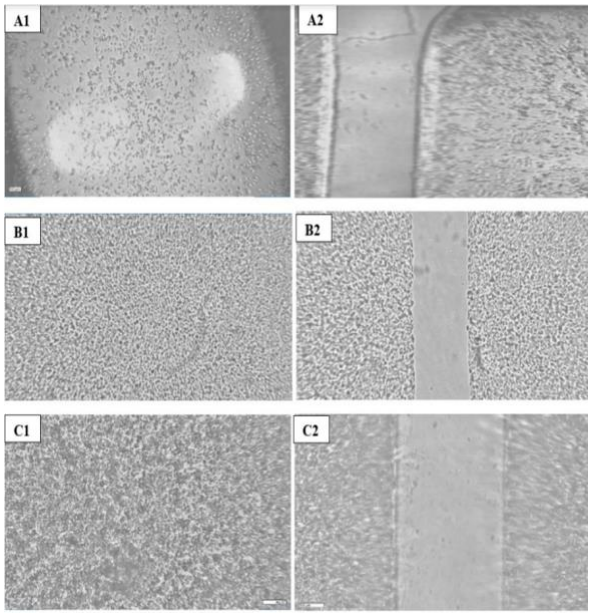

Figure 12**:** Optimization of the amount of Hela cells to be seeded in the 2 well Ibidi inserts.
Images taken with the Lonza software 24 hrs after seeding. In (A1) and (A2) 70 000 cells were seeded per well which was not enough as there is a lot of space between the cells which is not ideal to obtain a free cell gap. In (C1) and (C2) 300 000 were seeded per well which was too confluent after 24 hrs and cells were growing on top of each other thus competing for nutrients causing most cells to die and detach from the surface of the plate. In addition, it can clearly be seen that some cells passed inside the gap area. In (B1) and (B2) 100 000 cells were seeded per wells and this seemed to be ideal as cells had enough room to attach to the surface of the plate and cells did not pass through gap and created a free cell gap upon removal of the insert after 24 hrs.

3.4.5. Invasion assay

For this assay we used invasion assay inserts with a pore PET membrane of 8 µm, see Figure 13 (Falcon, USA). Our first goal was to optimize the number of cells to plate, optimize the protocol and the cell counting method, (see 3.4.6. below). In the sterile BSC, the Geltrex (Gibco, USA) and pipette tips were put on ice before starting the experiment. First, 50 µL of Geltrex was added into the upper invasion chamber of the well insert, which was placed inside a 24 transwell plate and subsequently placed in the incubator for 30 min to allow the Geltrex to solidify. After, 100 µL of serum free media

containing 50 000 cells was added on top of the Geltrex in the upper chamber and 600 µL of competed RPMI was added into the 24 well plate cell culture plate (bottom chamber). The plate was placed in the incubator for 24 hrs to allow the cancer cells to invade. After 24 hrs, the invasion insert was washed in PBS twice. Cells were fixed with adding 600 µL of 4 percentage paraformaldehyde both to the invasion chamber and the 24 transwell plate for 10 minutes. The invasion insert was again washed with PBS twice and stained by adding 200 µL of Giemsa, straight from stock, (Merck, Germany) to the upper well and 500 µL dyes to the bottom chamber. The stain was incubated for 10 minutes. After, the invasion insert was washed twice in PBS and the upper layer of the invasion chamber was wiped with a wet cotton swab to remove cells that did not invade. The invasion well was left to dry for 24 hrs before using the Lonza system to take pictures of the migrated cells (10x magnification in 5 random fields). Using ImageJ, the total number of invaded cells was counted.

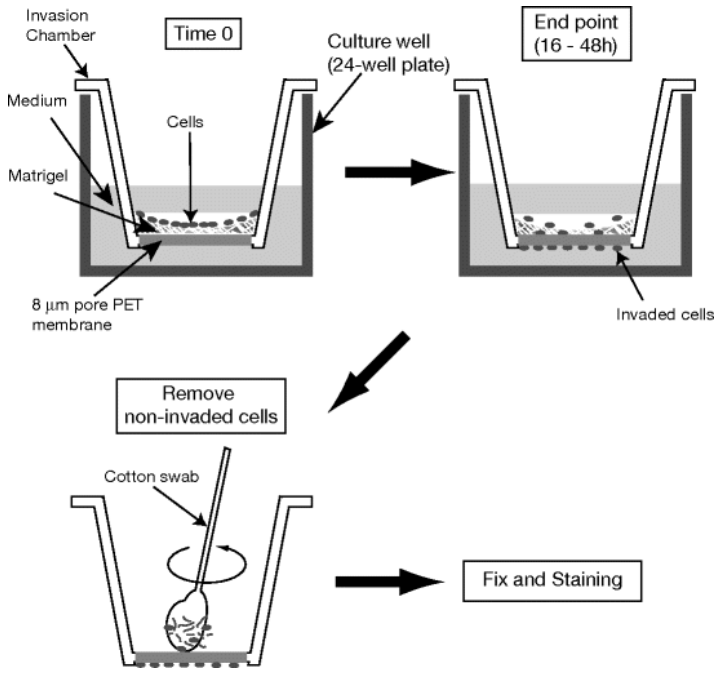

Figure 13**:** Workflow of the invasion assay using the well inserts with a pore PET membrane of 8 µm
(Palmisano and Itoh, 2010).

3.4.6. Optimization of the method to count the amount of invaded cells

To determine the total number of cells that passed through the membrane of the insert, the Lonza cytosmart live imaging camera was used to capture 5 random pictures after staining and the number of cells was quantified through image enhancement, geometric operation, colour processing editing and analysis using the ImageJ software. To achieve this, every picture was dragged into ImageJ and converted into a black and white image by changing its type to 16-bit. Subsequently, all particles that did not resemble cells were manually deleted using the eraser tool. Then a threshold was applied and it seemed ideal to adapt the lower and upper threshold to greater than zero but less than or equal to 175. This resulted in a white background with the cells highlighted in black (see Figure 14B) but this threshold had to be manually adapted depending on the background of the image to make sure all cells were counted. After, the watershed tool was applied to split touching cells. Finally, using the 'analyze particles tool' a range was applied between 10,15, 20, 25 and a maximum of 30 to infinity, to ensure all cells were counted, as shown in Figure 14C.

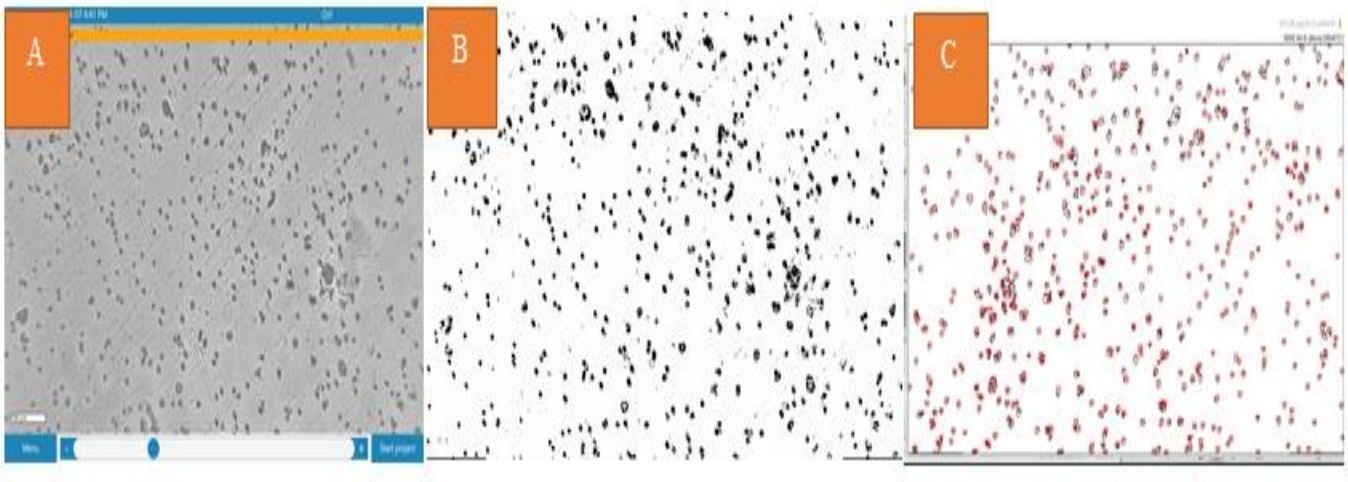

Figure 14**:** Conversion of the image using the ImageJ software and application of the `analyze particles` tool.
Image (A) shows an image taken of the bottom of the invasion insert using the Lonza cytosmart camera. Image (B) shows an image after applying the lower threshold of 100 and upper threshold of 161. Image (C) shows the image after applying 25-infinty for the analyze particles tool and all counted cells are highlighted in red. Image A and C were compared to evaluate if the threshold and analyzed particles tool was successful and if all cells were counted.

3.4.7. Apoptosis assay

When the cervical cancer cells had reached 60 percentage confluence in a T25 cell culture flask, the media was aspirated and transferred to a labelled centrifuge tube to collect any floating dead cells. The T25 cell culture flask was subsequently washed with 2 mL sterile PBS. Cells were detached after a 3 min incubation with 1 mL trypsin (0.5 x) or 1 mL accutase (Biolegend, UK) in the incubator. The optimal detaching method was optimized first. One (1) mL sterile PBS was added to the T25 flask to collect and transfer the cells to the labelled centrifuge tube (2X). The centrifuge tubes were centrifuged for 4 min at 900 rpm. The pellet was resuspended in 2 mL sterile PBS and the total amount of cells in every centrifuge tube counted. The cells were divided in several FACS tubes, depending on the experimental conditions tested. Ideally, each FACS tube should contain $1x10^6$ cells. The FACS tubes was centrifuged for 4 min at 900 rpm and the supernatant removed. The pellet was re-suspended in 100 µL binding buffer (BD Pharmingen, USA) (diluted binding buffer from 10X to 1X in distilled water) and 5 µL FITC annexin and 5 µL PI was added (BD Pharmingen, USA), followed by a gently mix and incubation in the dark for 15 min. After 15 min, 400 µL of binding buffer was added and the samples were read out using the BD Accuri 6 flow cytometer. The tubes were gently vortexed and analyzed with a medium speed until 35000 events were detected in P2. A backflush was performed between each sample. Finally, the percentage living, early and late apoptotic cells were determined.

Chapter 4: Results

The concentration of GI254023X was determined by the MTT assay, which was performed by Dr. Shankari Nair. The EC50 for the Hela cervical cancer cells was defined as 20.3 µM (20.3 µL stock solution per mL of (cRPMI)) and for C33A cervical cancer cells the EC50 was defined as 15.58 µM (15.58 µL stock solution per mL of (cEMEM)). Due to time and lab restrictions due the COVID19 pandemic, we decided to perform all selected assays using the Hela cervical cancer cells. We only used the C33A cervical cell lines for the CSA and Invasion assay. The C33A cells appeared to have a slow doubling time so it took longer to reach their exponential growth phase and we had issues with contamination.

4.1. Colony survival assay (CSA)

4.1.1. Results of the CSA using Hela cervical cancer cells

In Figure 15 a stained Hela colony is visualized three days after staining. A colony was counted if it was made up of minimum 50 cells.

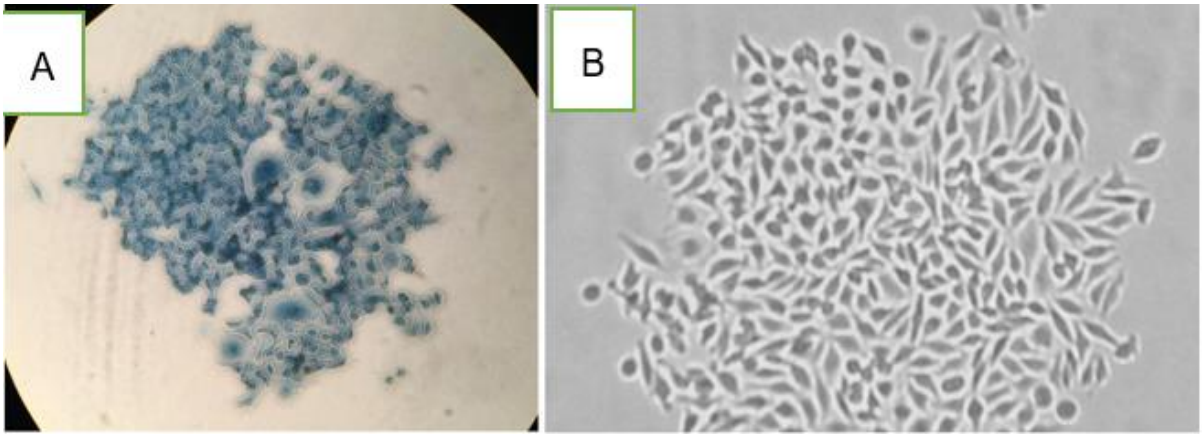

Figure 15**:** Stained Hela cervical cancer colony
(A) Picture of a Hela cell colony under a light microscope. (B) Image captured with the Lonza Cytosmart live imaging system.

The total survival fraction (SF) and standard deviations (SD) of the number of colonies counted for the Hela cervical cancer cells for 6 repeats per conditions are given in Table 6. The P-values of the Kruskal-Wallis test are added in the last column. The SF was compared between the three treatment conditions for every radiation dose using the GraphPad software. The GraphPad software was used for the statistical analysis of Kruskal-Wallis test , Mann-Whitney U and enhance visual graph customization.

Table 6**:** Survival fractions and results of the Kruskal-Wallis test of the CSA of the Hela cervical cancer cells.

Dose (Gy)	**IR**		**IR + 2 hrs GI**		**IR + 24 hrs GI**		**Kruskal-Wallis test P values**
	Mean SF	***SD***	***Mean SF***	***SD***	***Mean SF***	***SD***	
8	0.0293	0.0040	0.0449	0.0166	0.0292	0.0065	**0.0403***
6	0.0762	0.0057	0.1593	0.0265	0.1024	0.0098	**0.0005***
4	0.3149	0.0615	0.5919	0.0716	0.3788	0.0371	**0.0015***
2	0.5591	0.0929	1.0294	0.1354	0.7939	0.0751	**0.0011***
0	0.2309	0.0406	0.2092	0.0470	0.2095	0.0430	-----

Bold* = significant p value, IR = irradiation, Gy = gray, SD = standard deviation, SF = survival fraction

Based on the absolute values of the SF of Hela cervical cancer cells, when comparing IR to IR+2 hrs GI, there was an increase in the number of colonies when GI was added 2 hrs before irradiation for all radiation doses. This was also true when IR was compared to IR+24 hrs GI except for 8 Gy +24 hrs GI (SF 0.0292 versus 0.0293 for IR 8 Gy). When the absolute SFs were compared between IR with 2 hr GI incubation and 24 hrs GI incubation, it was clear that the longer the GI was added to the cells, there were less colonies produced. This was true for all dose conditions. When we applied the Kruskal-Wallis nonparametric test, a statistically significant different SF ($p < 0.05$) was shown between the three treatment conditions (IR only, IR + 2 hrs GI and IR + 24 hrs GI) for all IR doses: 8 Gy ($p = 0.0403$), 6 Gy ($p = 0.005$), and 4 Gy ($p = 0.0015$) and 2 Gy ($p = 0.0011$).

The P-values of the Mann-Whitney test are shown in Table 7 to determine if there were significant differences in the SFs of the Hela cells between the two different treatment

conditions. This was calculated using the GraphPad software, where only two conditions were compared to each other for each radiation dose.

Table 7: Results of the Mann-Whitney U test on the CSA data of the Hela cervical cancer cells.

Dose (Gy)	IR v/s IR + 2Hr GI	IR v/s IR + 24Hr GI	IR + 2Hr GI v/s IR + 24Hr GI
2	**0.0022***	**0.0022***	**0.0260***
4	**0.0022***	0.0649	**0.0022***
6	**0.0022***	**0.0022***	**0.0022***
8	**0.0152***	1	0.0649

Bold* = significant p value, IR = irradiation, Gy = gray, Not bold not significant, v/s Versus

If the SF of IR only was compared to IR + 2 hrs GI, there was a significant change when GI was added as the P value was less than 0.05 for each radiation dose 2 Gy ($p = 0.0022$), 4 Gy ($p = 0.0022$) 6 Gy ($p = 0.0022$) and 8 Gy ($p = 0.0152$). When IR only was compared to IR+ 24 hrs, GI there was only a significant increase for 2 Gy ($p = 0.0022$) and 6 Gy ($p = 0.0022$). If the SF of IR + 2 hrs GI were compared to IR + 24 hrs GI the P value was significant for 2 Gy ($p = 0.0260$), 4 Gy ($p = 0.0022$) and 6 Gy ($p = 0.002$), where the 24 hrs incubation leads to lower SFs.

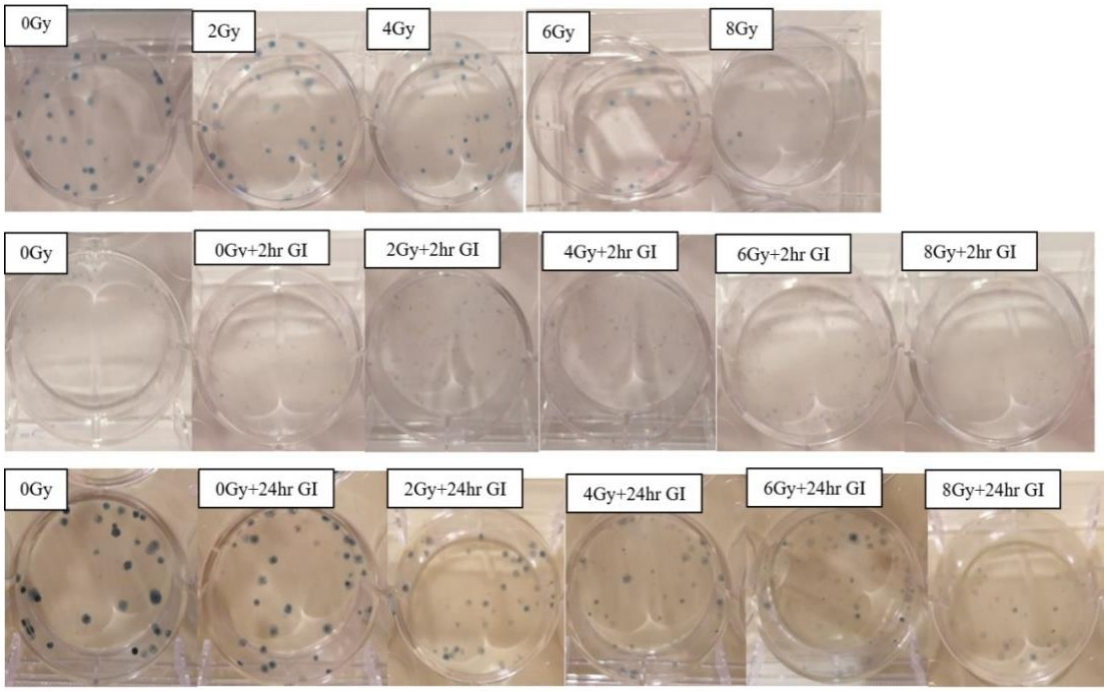

Figure 16**:** Images of the CSA of Hela cervical cancer cells after irradiation or irradiation combined with GI therapy.
The number of colonies was manually counted after staining to determine the (SF) (6 repeats for each condition). 1st row represents the condition IR only, the 2nd row is IR + 2 hrs GI and the 3rd row is IR + 24 hrs GI. A colony was counted if it was made up of minimum 50 cells.

Figure 16 shows images of the colonies that were counted for this experiment. For the 2nd condition (IR + 2 hrs GI), the colonies were less visible. Whereas the colonies of the 3rd condition (IR + 2 hrs GI) and 1st condition (IR + 24 hrs GI) colonies were clearly visible. We normalized the data to determine the SF for this assay.

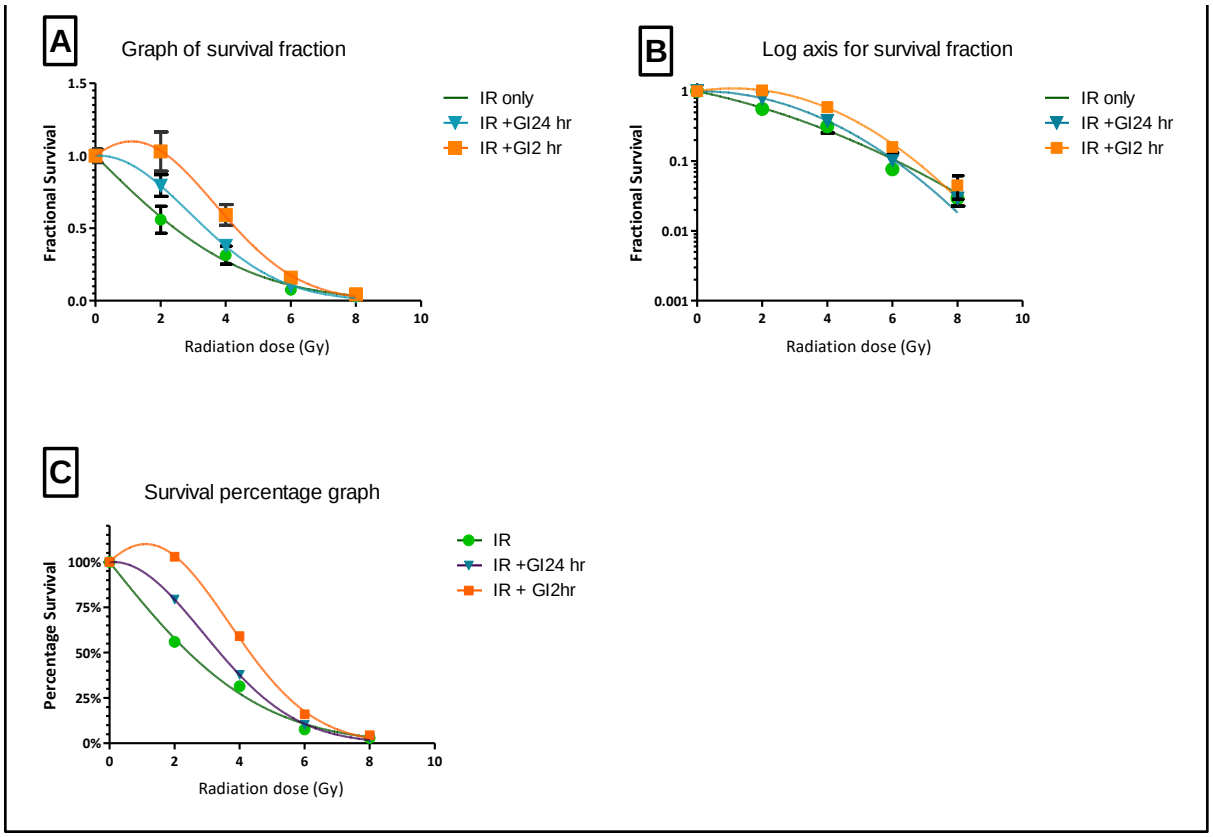

Figure 17**:** CSA data of Hela cervical cancer cells.
Hela cervical cancer cells, Graph (A) shows the survival fraction vs the radiation dose. Graph (B) shows the log axis of the survival fraction vs the radiation dose. Graph (C) represents the percentage of the survival fraction vs the radiation dose.

From the graph, it is clear that the SF of the cells decreased as the levels of radiation increased but the rate of the decrease was different for the IR only compared to the IR + 2 hrs GI and IR + 24 hrs GI. It can also be seen from the graphs that there was no increased rate of cells death when GI was added to the cells. This can also be seen in Table 6, where the SF of IR was less than that of IR + 24 hrs GI and IR + 2 hrs GI. However, if (IR + 2Gy) were compared to (IR + 24 hrs GI), the SFs were significantly lower at 2, 4 and 6Gy if GI was added 24 hrs compared to 2 hrs.

4.1.2. Results of the CSA using C33A cervical cancer cells

The total SFs and SDs of the number of colonies counted for the C33A cervical cancer cells for 6 repeats per conditions are given in Table 8. The P-values of the Kruskal-

Wallis test were added in the last column. The SF was compared between the three treatment conditions for every radiation dose using the GraphPad software.

Table 8**:** Survival fractions and results of the Kruskal-Wallis test of the CSA of the C33A cervical cancer cells.

Dose (Gy)	**IR**		**IR+ 2hr GI**		**IR + 24hr GI**		**Kruskal-Wallis test P value**
	Mean SF	***SD***	***Mean SF***	***SD***	***Mean SF***	***SD***	
8	0.0009	0.0002	0.0008	0.0008	0.0042	0.0012	**0.031***
6	0.0092	0.0014	0.0027	0.0028	0.0410	0.0085	**0.0005***
4	0.0765	0.0146	0.0453	0.0290	0.0900	0.0154	**0.0240***
2	0.4104	0.0590	0.3792	0.0714	0.3713	0.0523	0.5805
0	0.6497	0.0616	0.1938	0.0228	0.4638	0.0310	

Bold* = significant p value, IR = irradiation, Gy = gray, SD = standard deviation, SF = survival fraction

When comparing the absolute values of the SF between IR only and IR + 2 hrs GI, a decrease in the number of colonies was seen when GI was added 2 hrs before irradiation for all radiation doses. This was not true when IR was compared to IR + 24 hrs GI, where there were more colonies when GI was added except for 2 Gy + 24 hrs GI, where the mean SF was 0.3714, while 2 Gy only had a SF of 0.0410. When the SFs of IR + 2 hrs GI were compared to IR + 24 hrs GI, it was clear that the longer GI was added to the cells, the more colonies were produced when GI was added for 24 hrs, except for 2 Gy. Statistically significant differences in SFs between the three treatment groups was found for 8 Gy ($p = 0.031$), 6 Gy ($p = 0.005$), and 4 Gy ($p = 0.0240$) but not for 2 Gy ($p = 0.5805$).

The P-values of the Mann-Whitney U test are shown in Table 9 to determine if there were significant differences in the SFs of the C33A cells between the two different treatment conditions. This was calculated using the GraphPad software, where only two conditions were compared to each other for each radiation dose.

Table 9**:** Results of the Mann-Whitney U test on the CSA data of the C33A cervical cancer cells.

Dose (Gy)	IR v/s IR + 2Hr GI	IR v/s IR + 24Hr GI	IR + 2Hr v/s IR + 24Hr GI
2	0.4848	0.3939	0.9372
4	**0.0411***	0.1797	**0.0304***
6	**0.005***	**0.005***	**0.0048***
8	0.6868	**0.0048***	**0.0047***

Bold* = significant p value, IR = irradiation, Gy = gray, Not bold not significant, v/s Versus

When IR only was compared to IR + 2 hrs GI, there was a significant decrease in SF when GI was added when irradiated with 4 Gy (p = 0.0411) and 6 Gy (p = 0.005). When IR only was compared to IR+ 24 hrs GI, there was only a significant increase in SF at 6 Gy (p = 0.005) and 8 Gy (p = 0.0048). When IR + 2 hrs GI was compared to IR + 24 hrs GI, the value of P was significant for 4 Gy (p = 0.0304), 6 Gy (p = 0.0048) and 8 Gy (p = 0.0047), where the 24 hrs incubation resulted in higher SFs compared to the 2 hrs incubation.

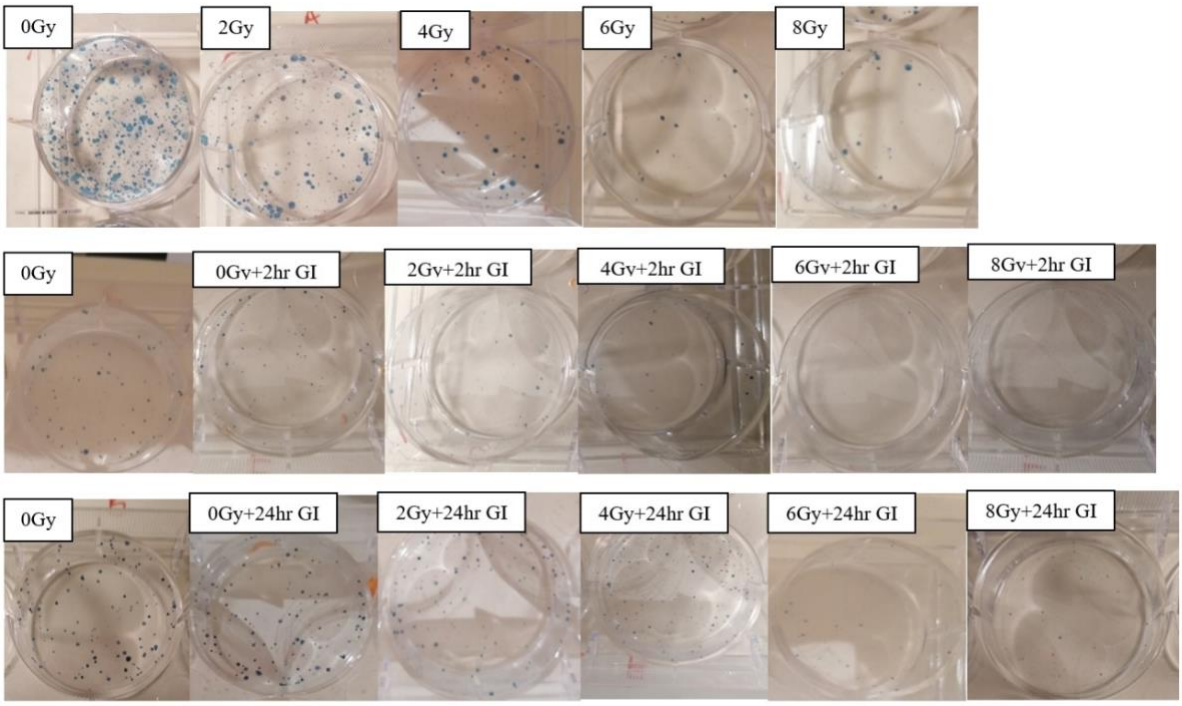

Figure 18**:** Images of the CSA assay of C33A cervical cancer cells after irradiation or combined irradiation with GI therapy.
The colonies counted to define the SF of the C33A cervical cancer cells consisted of a minimum of 50 cells. The SF was defined for 6 repeats for each condition. 1st row is for IR only, 2nd row is IR + 2 hrs GI and 3rd is for IR + 24 hrs GI.

Figure 18 shows images of the colonies that were counted for this experiment. For the 2nd condition (IR + 2 hrs GI), less colonies were visible. Whereas the colonies of the 3rd condition (IR +2 hrs GI) and 1st condition (IR + 24 hrs GI) were clearly visible. We normalized data to determine the SF for this assay.

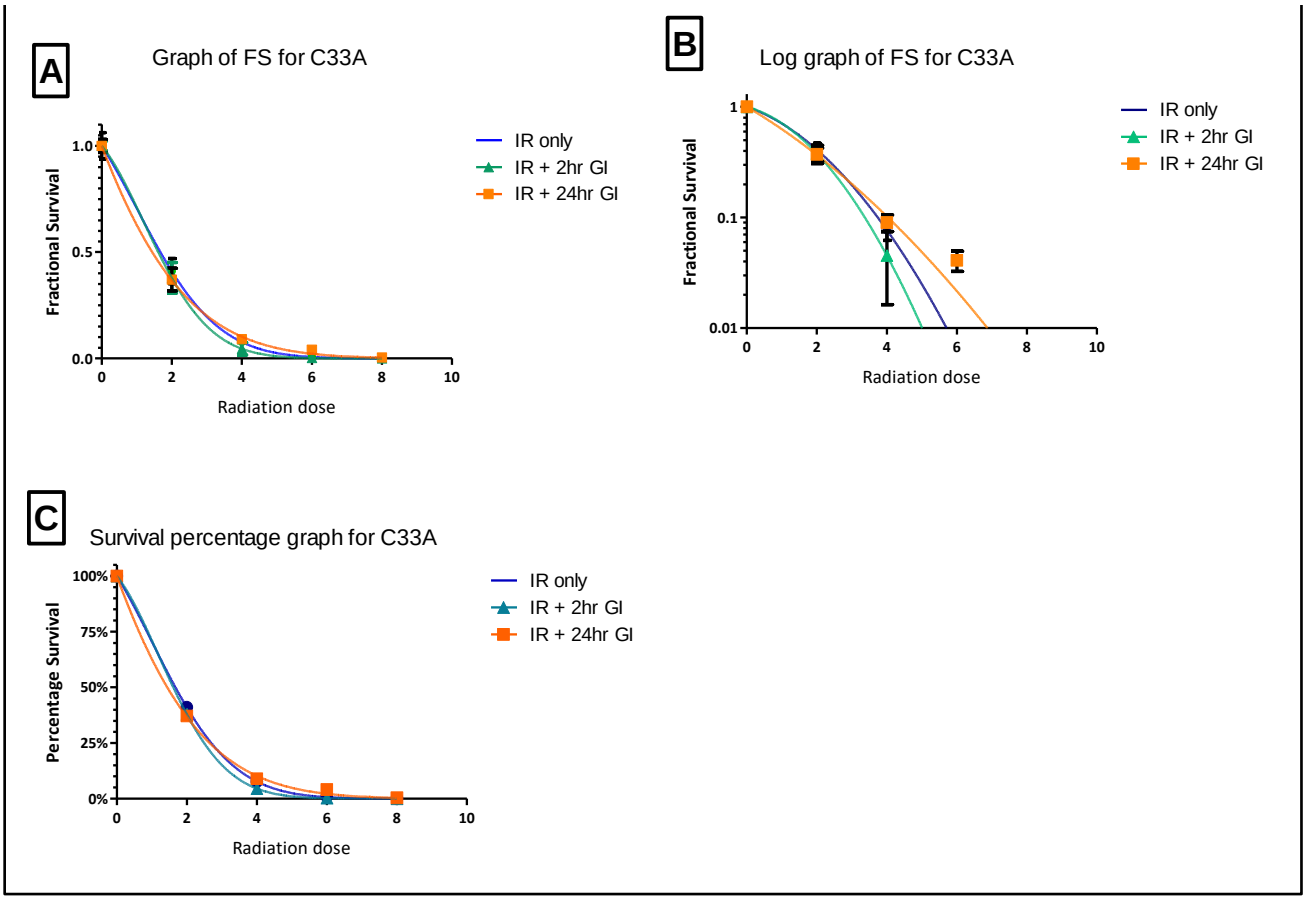

Figure 19**:** CSA data of the C33A cervical cancer cells.
C33A cervical cancer cells. Graph (A) shows the survival fraction vs the radiation dose. Graph (B) shows the log of the survival fraction vs the radiation dose. Graph (C) represents the percentage of the survival fraction vs the radiation dose.

From the graphs of the SF of the cells, for all conditions, a decrease was visible when the radiation dose increased but the rate of the decrease was comparable between the different treatment conditions. However, in graph B, a slight increased rate of cell death due to the addition of GI 2 hrs before irradiation compared to IR only could be seen. This was, however, the opposite for the condition, where GI was added 24 hrs before irradiation. This could also be seen in Table 8, where the SF of IR +2 hrs GI was less than IR only.

4.2. Migration – wound healing assay

The migration assay was only performed with the Hela cervical cancer cells due to the time limit and lab restrictions caused by the COVID19 pandemic.

4.2.1. Results of the migration assay for the Hela cervical cancer cells

Twenty four (24) hours after seeding of the cells in the Ibidi wells, the Ibidi insert was removed and the cells attached to the surface of the cell culture micro-dishes were washed with media and 2 mL of fresh media was added. Using the Lonza Cytosmart live imaging system, the field of view was focused on the gap and snapshots were taken every 15 min upon closure of the gap (inside the incubator). Table 10 shows the percentage of the gap area, which was calculated using the automatic algorithms of the Cytosmart app. The percentage gap closure was calculated relative to the gap area at the starting time point, put as 100 percentages. The speed of gap closure was calculated automatically using the algorithms of the Cytosmart app.

Table 10**:** Hela cervical cancer cell migration assay results.

time (min)	control	2Gy	GI only	2Gy + GI
% gap area				
0	100.00	100.00	100.00	100.00
195	89.61	85.54	85.70	87.43
345	59.28	57.19	65.64	60.86
495	25.78	27.13	42.80	37.29
705	0.00	1.75	20.38	15.60
855	0.00	0.00	9.08	8.06
1005	0.00	0.00	2.61	4.96
1155	0.00	0.00	0.36	0.00
1245	0.00	0.00	0.00	0.00
% gap closure				
0	0.00	0.00	0.00	0.00
195	10.39	14.46	14.30	12.57
345	40.72	42.81	34.36	39.14
495	74.22	72.87	57.20	62.71
705	100.00	98.25	79.62	84.40
855	100.00	100.00	90.92	91.94
1005	100.00	100.00	97.39	95.04
1155	100.00	100.00	99.64	100.00
1245	100.00	100.00	100.00	100.00
Speed closure				
0	0.00	0.00	0.00	0.00
195	-55.68	-2.88	-51.90	-53.93
345	-13.27	16.08	-11.39	-21.96
495	3.76	19.67	-15.36	-14.45
705	1.42	12.96	-1.41	7.80
855	0.00	0.00	1.71	-2.13
1005	1.17	0.00	1.52	0.50
1155	0.00	0.00	0.46	0.00
1245	0.00	0.00	1.59	0.00

For this experiment, only 1 run was completed per condition. In the control condition, the gap was closed at 705 min, after 2 Gy irradiation at 855 min, after GI treatment only at 1245 min and at the combined treatment (2 Gy +GI) at 1155 min after the removal of the Ibidi well. This shows that GI, radiation or combined treatment all had an effect on the rate of the migration of the Hela cells.

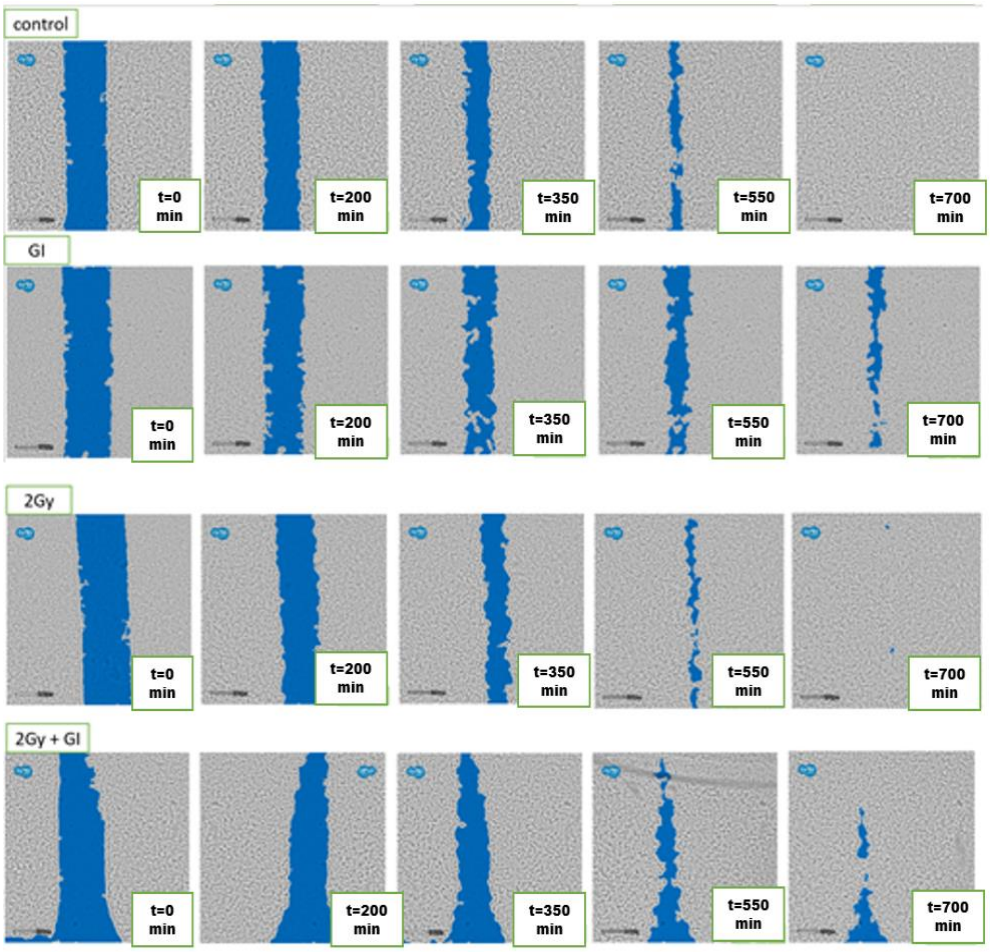

Figure 20**:** Migration images captured using the Lonza cytosmart live imaging system. *The blue area represents the area of the gap, which was automatically calculated using the Cytosmart gap area algorithm at different time points (0, 200, 350, 550 and 700 min) for every treatment condition (control, GI only, 2 Gy and 2 Gy + GI). Visually you can see that the conditions including GI slowed down the gap closure.*

Figure 20 shows the time intervals of the migration assay for the four different treatment conditions using the Lonza imaging system. Multiple images of the gap, highlighted in blue, were taken for specific times (every 15 minutes during 24 hrs). From the Figure 20 and Table 10, it can be seen that GI or combined therapy had an effect on the rate of gap closure, where it took longer for the gap to close confirming a migration inhibition effect.

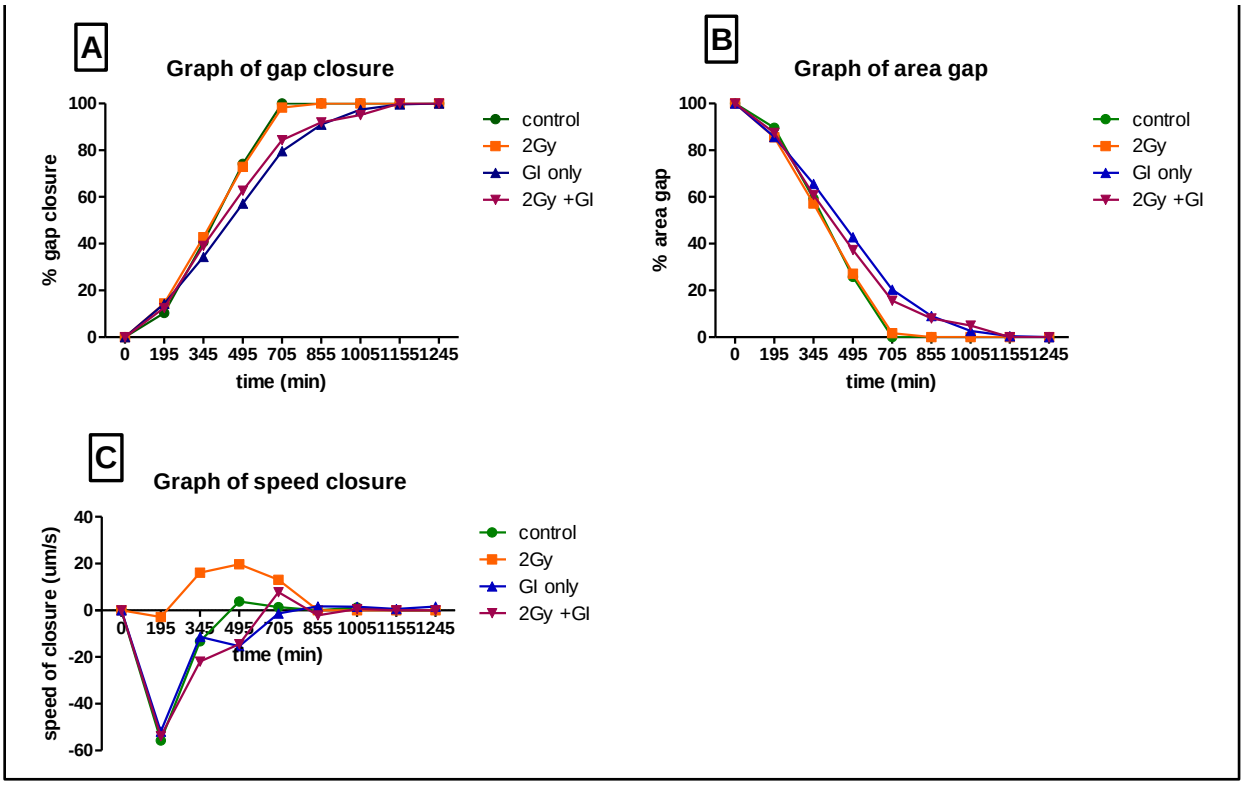

Figure 21**:** Graph of wound healing for Hela cervical cancer cells.
Graph (A) shows the percentage gap closure in function of the time. Graph (B) shows the area of the gap in function of the time. Graph (C) shows the wound healing speed in function of the time.

Since we had only 1 repeat per condition, no statistics was performed. Only a trend was discussed based on the graphs. From the graph, it can be seen that compared to controls there was an increase in the time to reach 100 percentage gap closures when treated with GI and combined treatment. The time of gap closure for 2 Gy and control was 855 and 705, respectively, but from the graph of Figure 21 A and B, the two curves were overlapping each other. Interestingly, it can be seen in graph C that the speed closure of the 2 Gy condition (orange) was higher compared to the other conditions.

4.3. Invasion assay

For this invasion assay, 50 000 cells in serum-free media were plated in the insert pre-incubated with 50 µL of Geltrex. Due to time and lab restrictions from to the COVID19 pandemic, only 4 invasion wells were completed for the C33A cervical cancer cells.

4.3.1. Results of the invasion assay of Hela cervical cancer cells

Three (3) repeats were done with Hela cervical cancer cells for each condition to get a mean and SD of the number of invaded cells. The mean of the total number of cells that had passed through the PET membrane of the chamber was a mean from 5 fields of views taken with the Lonza software of the same invasion insert membrane.

Table 11**:** Mean, standard deviation and Kruskal-Wallis test of invasion data of the Hela cervical cancer cells.

Sample	Mean ± SD	Mean of invaded cells per condition
Control 1	521.2 ± 17.53	534.6 ± 23.47
Control 2	525.2 ± 27.62	
Control 3	557.2 ± 25.26	
2Gy 1	562.4 ± 65.57	583.5 ± 65.50
2Gy 2	616 ± 89.83	
2Gy 3	572 ± 41.09	
2Gy + GI 1	530.8 ± 41.11	544.9 ± 26.87
2Gy + GI 2	505.2 ± 12.97	
2Gy + GI 3	598.8 ± 26.53	
GI 1	485.8 ± 58.26	547.9 ± 93.17
GI 2	556.4 ± 28.15	
GI3	601.6 ± 193.10	
Kruskal-Wallis test	0.3466	

Bold* = significant p value, SD = standard deviation, Not bold not significant

The more cells passed through the PET membrane, the less effective treatment was at inhibiting invasion. From Table 11 and Figure 22, there was no clear difference in cell count. The mean and standard deviation showed that the number of invaded cells fell under the same range. The value for P was greater than 0.05 thus the use of GI did not have a significant effect on the invasion of the cells. It can also be seen that the standard deviations for control with 2Gy + GI and that of 2 Gy and GI only overlap.

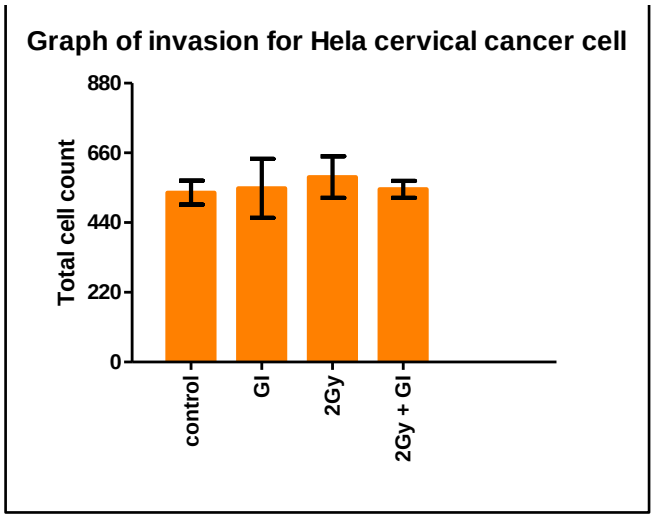

Figure 22**:** Graph of invasion assay results of Hela cervical cancer cells
Shows the number of cells that has passed through the PET membrane for the 4 different treatment conditions.

The P-values of the Mann-Whitney U test are shown in Table 12 to determine if there were significant differences in the amount of invaded Hela cervical cancer cells between the two different treatment conditions. This was calculated using the GraphPad software, where only two conditions were compared to each other for each radiation dose.

Table 12**:** Mann-Whitney U test comparing the amount of invaded Hela cervical cancer cells between the different treatment conditions.

Comparison	**p-value**
Control vs GI	1.000
Control vs 2 Gy	0.1000
Control vs 2 Gy + GI	1.000
2 Gy vs 2 Gy + GI	0.3006
GI vs 2 Gy	0.4000
GI vs 2 Gy + GI	1.000

Bold* = significant p values (<0.05)

The P-values for all the comparisons made (Table 12) were greater than 0.05 and hence not significant. Hence, we could conclude that there was no invasion inhibition induced by the GI drug.

4.3.2. Results of the invasion assay of the C33A cells

The mean of the total number of cells that passed through the PET membrane of the chamber was a mean from 5 fields of views taken with the Lonza software of the same invasion insert membrane. The invasion assay with C33A cervical cancer cells was performed two times for each condition.

Table 13**:** Mean and standard deviation of invasion data of C33A cervical cancer cells.

Sample	Mean ± SD	Mean of invaded cells per condition
Control 1	467.8 ± 78.08	532.4 ± 70.10
Control 2	597.0 ± 70.12	
2Gy 1	531.2 ± 42.70	526.4 ± 34.95
2Gy 2	521.6 ± 27.19	

SD = standard deviation

From the Table 13, the mean of the invaded cells ranged around 520 for both treatment conditions and the standard deviation was overlapping, showing that there was no different in invasion due to treatment. This can also be seen in Figure 23.

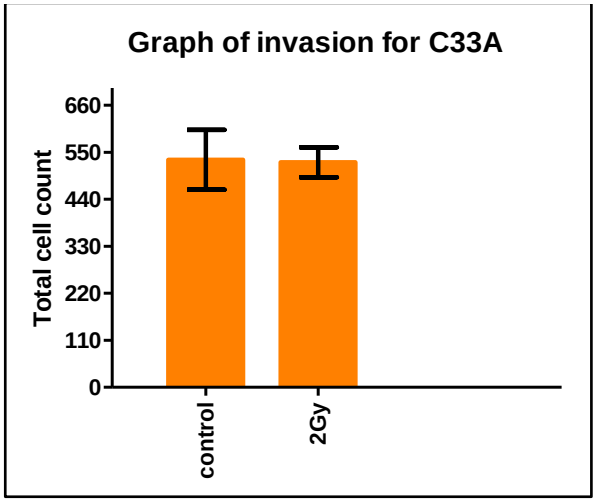

Figure 23**:** Graph of invasion assay results of C33A cervical cancer cells**.**
The graph shows the number of cells that passed through the PET membrane for the 2 different treatment conditions for C33A cervical cancer cells.

4.4. Apoptosis assay

For this assay, only Hela cervical cancer cells were used due to time limits, lab restrictions and slow growing C33A cells, where the C33A needed more time for them to reach exponential growth.

4.4.1. Comparison of trypsin versus accutase for detaching Hela cervical cancer cells

Trypsin was compared to accutase to see which one had a less damaging effect for the detachment of healthy cervical cancer cells. The effect of trypsin and accutase to detach the cells from the surface of the cell culture flask was compared since a high concentration of trypsin is known to cause damage to the cell membrane of the cells, resulting in binding of the annexin to the cell membrane. This can result in a lower number of living cells and a higher number of early apoptotic cells, which was not related to the applied treatment. In this experiment, the concentration of trypsin was decreased from 2X to 0.5X and compared to a less toxic detachment enzyme accutase.

Table 14**:** Apoptotic fractions induced by trypsin versus accutase for detaching Hela cervical cancer cells.

Sample name	**Living**	**Early apoptotic**	**Late apoptotic**	**Mean apoptotic**
Trypsin 1	92.1 %	2.88 %	4.72 %	7.60 %
Trypsin 2	92.57 %	3.26 %	3.81 %	7.07 %
Trypsin 3	91.83 %	3.28 %	4.60 %	7.88 %
Mean	92.09 %	3.26 %	4.60 %	7.60 %
SD	0.38 %	0.22 %	0.49 %	0.42 %
Accutase 1	90.55 %	3.24 %	5.85 %	9.09 %
Accutase 2	90.41 %	3.34 %	5.96 %	9.30 %
Accutase 3	90.33 %	2.63 %	6.13 %	8.76 %
Mean	90.41 %	3.24 %	5.96 %	9.09 %
SD	0.11 %	0.38 %	0.14 %	0.27 %
Mann-Whitney U p-value	**0.10**	**1.00**	**0.10**	**0.10**

By looking at the absolute values, it could be seen that the mean percentage of the living was 1.68 lower, the mean early apoptosis was 0.02 higher and late apoptosis was 1.36 higher for cells that were loosened with accutase compared to those loosened with trypsin. These differences were not statistically significant as seen from the p-values determined in Table 14. The percentage difference in total apoptosis (early + late apoptosis) was 1.49 and even if not significant, trypsin 0.5X was selected for future experiments. The P values for Hela cervical cancer cells for trypsin (n = 3) in comparison to accutase (n = 3) for the amount of living cells was 0.1, early apoptosis was 1 and late apoptosis was 0.1, which were greater than 0.05, thus there was no significant difference between the use of accutase or trypsin for detachment. Even if not significant, the absolute values showed that trypsin had more living cells and less cells in the apoptotic stage thus for this experiment, trypsin was used for detachment due to its ability to be less damaging to the cell membranes of cervical cancer cells.

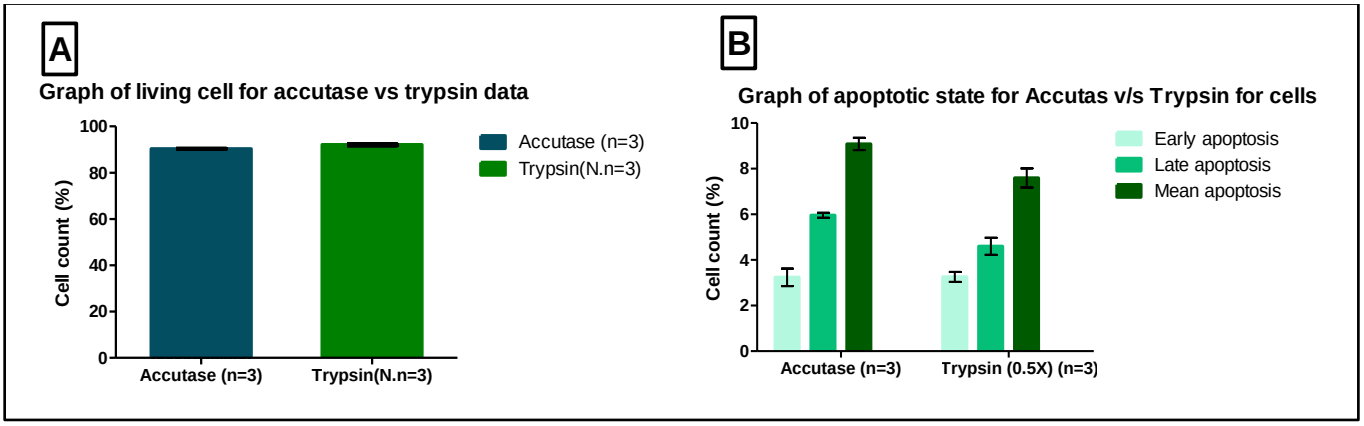

Figure 24**:** Graph of apoptotic fractions after detaching Hela cells with accutase versus trypsin (0.5X).
Graph shows the number of cells counted in the 3 different stages. In graph (A) the number of living cells is not significantly different between trypsin and accutase. In graph (B) there are a higher number of cells in apoptotic stages for accutase than for trypsin, however this difference is not statistically significant.

4.4.2. Establishment of the template for apoptosis analysis of the Hela cells

Determination of the distribution of the scattering of light (side scattering and forward scattering) was based on the state of the cell in a living, early and late apoptotic state. PI would enter the cell if damaged and annexin would attach to the cell membrane, which would cause light to be scattered and reflected to be able to determine the status

of the cell. The template would be used for the determination of percentage living, early and late apoptotic cells in every sample. To create the template, we compared single and/or double annexin and PI staining between healthy and dead cells (achieved by placing cells in 70℃ for 10 minutes), see Figure 25.

Table 15: Results of the annexin / PI template optimization experiment of Hela cervical cancer cells.

Sample name	Living	Early apoptotic	Late apoptotic
Healthy No AB	99.98 %	0.00 %	0.01 %
Healthy PI only	91.45 %	0.00 %	0.01 %
Healthy Ann only	88.01 %	11.97 %	0.00 %
Healthy Ann + PI	88.21 %	4.13 %	7.43 %
Dead No AB	99.97 %	0.01 %	0.01 %
Dead PI only	0.56 %	0.00 %	0.03 %
Dead Ann only	0.21 %	99.79 %	0.01 %
Dead Ann + PI	0.92 %	1.03 %	97.98 %

AB = antibody (PI or annexin), Ann = Annexin

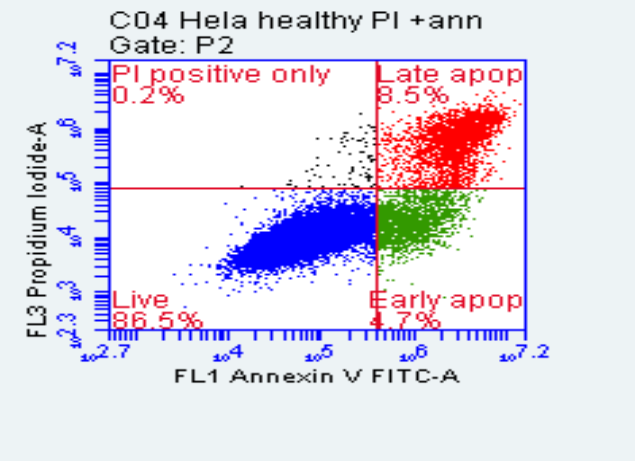

Figure 25**:** Optimized template for apoptosis analysis using the Annexin V/PI assay.
Blue = living cells, Red = late apoptosis, Black = PI only, Green = Early apoptosis.
To achieve this, dead and healthy Hela cervical cancer cell were used, where the dead cells were achieved by placing cells in water at temperature of 70 °C for 10 minutes and healthy cell are cells that have not been exposed to any treatment.

Template formed showed the distribution of the cells using a flow cytometry (BD Accuri C6 flow cytometer), where the region of scattering was picked up and compared between all 8 conditions shown in Table 15. This template was applied for all experiments with the therapeutic conditions.

4.4.3. Results of the apoptosis assay with Hela cervical cancer cells

The results of the apoptosis assay after treating Hela cervical cancer cells with different conditions was given in Table 16. Using the template, we determined the number of cells in the three different states (living, early or late apoptosis) to determine if the addition of GI and/or IR could induce more cell death.

Table 16**:** Mean and standard deviations of the apoptosis assay of Hela cervical cancer cells.

Sample name	Mean live ± SD	Mean early apoptosis ± SD	Mean late apoptosis ± SD
control (n = 4)	91.85 ±1.15	1.38 ± 0.45	6.14 ± 1.44
GI only (n = 3)	91.05 ±0.53	1.97 ± 0.16	6.42 ± 0.37
2 Gy (n = 3)	88.99 ± 2.04	1.8 0±0 .65	8.09 ± 2.35
8 Gy (n = 3)	86.91 ± 3.98	2.0 4± 0.52	9.89 ± 3.95
2 Gy + GI (n = 3)	86.18 ± 3.09	2.76 ± 0.53	10.22 ± 2.75
8 Gy + GI (n = 3)	83.06 ± 1.54	2.69 ± 1.38	12.84 ± 2.67

The P-values of the Mann-Whitney test are shown in Table 17 to determine if there were any significant differences in the amount of living, early apoptotic and late apoptotic Hela cells between the treatment conditions. This was calculated using the GraphPad software.

Table 17**:** Mann-Whitney U test of the apoptosis results of the Hela cervical cancer cells.

Sample name	p-value			
	Living cells	**Early apoptosis**	**Late apoptosis**	**Mean apoptosis**
Control / GI	0.4	0.1143	0.4	0.4
Control / 2 Gy	0.1143	0.4	0.2286	0.1143
Control / 2 Gy + GI	0.0571#	0.0571#	0.4	0.0571#
Control / 8 Gy	0.0571#	0.1536	0.0571#	0.0571#
Control / 8 Gy + GI	0.0571#	0.1143	0.0571#	0.0571#
2 Gy / 2 Gy + GI	0.7	0.2	1	0.7
8 Gy / 8 Gy + GI	0.7	1	1	0.7
GI / 2 Gy	0.4	1	0.7	0.2

Bold* = significant p value, # = borderline significant p value

It can be seen from Table 16 and Figure 26 that there was a change in the number of cells in the three different states for the 8 conditions, where there was an increase in the number of cells in early and late apoptosis as the level of radiation increased and when the GI drug was added. Also, when GI was used in comparison to the control, there were more living cells for the control and more cells in apoptosis state for GI, showing that GI could increase the number of cells going through apoptosis. This was also true when 2 Gy only was compared to 2 Gy + GI and 8 Gy only compared to 8 Gy + GI. However, when looking at the p-values in Table 17, it can be seen that only some p-values were borderline and significant at 0.0571 for the control vs 2 Gy + GI, control vs 8 Gy and control vs 8 Gy + GI for living cells; control vs 2 Gy + GI for early apoptosis, control vs 8 Gy and control vs 8 Gy + GI for late apoptosis and finally for control vs 2 Gy + GI, control vs 8 Gy and control vs 8 Gy + GI for mean apoptosis. Borderline significant means that the p-value was not small enough to claim statistical significance, but still was close enough to 0.05 to be worth mentioning. Interestingly, a trend was seen to increased apoptosis of Hela cells when control was compared to 2 Gy + GI, which was not visible when control was compared with 2 Gy only, showing a potential radiosensitizing effect ($p = 0.0517$). However, when 2 Gy was compared to 2 Gy + GI, no significant differences were seen in living or apoptotic cells.

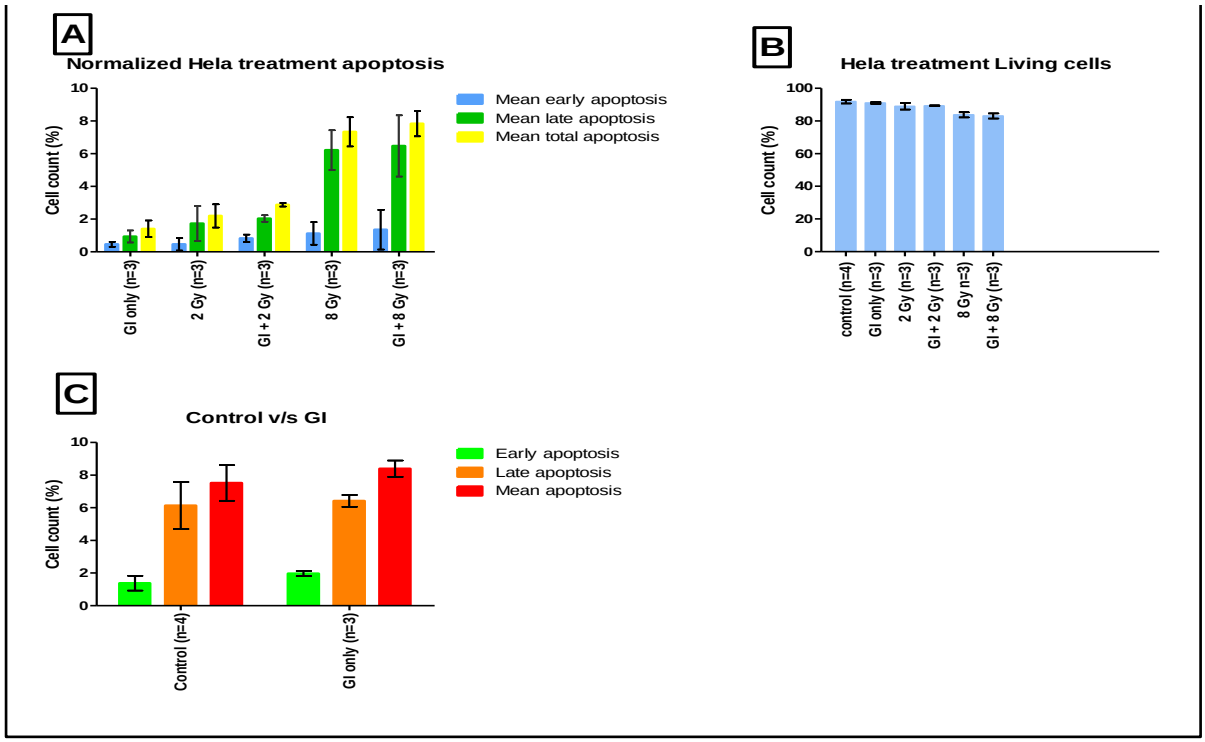

Figure 26**:** Graph of the apoptosis results of Hela cervical cancer cells.
Graph (A) show the percentage of cells in apoptotic states compared between the 6 different conditions. Graph (B) shows the percentage of living cells compared between the 6 different conditions. Graph (C) shows the percentage of cells in apoptotic state in controls versus GI only.

Chapter 5: Discussion and conclusion

5.1. Discussion

In this dissertation, we investigated the effect of an ADAM10 inhibitor on the proliferation, migration, invasion and apoptosis of cervical cancer cells, with and without combined radiation. The CSA was used to measure the ability of a cell to retain its proliferation ability over a period of time, which can be affected by the use of drug, radiation or combined therapy. It could be seen for the Hela cervical cancer cells that there was an increase in the number of colonies formed when GI was combined with radiation compared to irradiation only. This could mean that GI increased the formation of colonies instead of decreasing (see Table 6). However, when 2 hrs GI incubation was compared to 24 hrs incubation of GI before radiotherapy, the longer incubation time of GI in cells, decreased the colony formation. For the C33A (see Table 8), there were more colonies formed for IR + 24 hrs GI than in IR only, except at 2 Gy but there were less colonies produced when IR + 2 hrs GI was compared to IR only. These results were contradictive and we concluded that the experiment be repeated in the future to confirm the effect of GI on colony formation. Taken into consideration the change of media that took place right before irradiation of the samples for the IR + 2 hrs GI and IR + 24 hrs GI could also have affected the numbers of colony formation as the media was not changed for IR only condition. This action could have given cells new nutrients, causing them to grow and multiply better in fresh media thus resulting in more colonies formed when GI was added as was seen for the Hela.

We successfully optimized the migration assay for cervical cancer cells, as shown in Figure 12. The optimal number of cells to plate to ensure confluence and an ideal gap creation after 24 hrs was 100 000 cells per well. We also confirmed that the Ibidi wells could be reused by washing them with 70 percentage ethanol, autoclaving them and placing them under a UV light in the BSC for 10 min before use. However, this did affect the attachment of the Ibidi well to the microdish and could possibly influence the quality of the gap. For the migration assay, no statistics were performed as we did not have biological repeats for each experimental condition thus only the difference in gap closure of 1 run was compared. The time it took for the gap to close after treatment for

control, IR only, GI drug only or combined treatment was different for each condition and showed that GI and GI + radiation had an effect on the Hela cervical cancer cell migration rate. Interestingly, the time to reach gap closure was slightly longer for GI only (1245 min) compared to GI + 2 Gy, which was (1155 min), indicating that the combined therapy was not more effective at inhibiting migration as seen in Table 10 and Figure 20.

Secondly, we successfully optimized the invasion assay and the cell counting method. The invasion of cancer cells was defined based on their ability to pass through the membrane at the bottom of the insert since they were attracted to the serum in the media in the bottom well (no nutrients were available in the media where the cells were seeded in). A membrane of 8 µM was used since this was the optimal pore size to study the invasion of cancer cells (Kahl, 2020, Su et al., 2012). It is important to know that for the counting of images; the images were randomized (treatment condition was hidden to prevent bias). The results showed that more cells invaded after a 2 Gy irradiation compared to controls, indicating that the RT slightly increased the invasive potential of the cells although this difference was not significant. The results in Table 11 showed that the mean of the number of invaded cells was within the same range and the standard deviation overlaps for all treatment conditions. Based on these results, it could be said that the addition of GI did not affect the invasion of the cells. This could also be seen in the p-values, which were greater than 0.05. The P-values for the C33A data could not be determined since only 2 repeats per condition were performed. Concerning the counting method and image conversion, it was important to know that two thresholds were defined manually for each image that was counted. The first threshold defined the pixel to noise ratio while the second threshold in the analyzed particles tool was based on the size of the particles. Due to difference in background and noise of the pictures, applying the same threshold could lead to the missing up of cells in the counting. We noted that adapting the range of infinity in the analyze particles tool allowed to optimize the counting. To reach optimal counting, the original images were always compared to the counted ones to confirm if counting was performed correctly (Cavicchi et al., 2017). However, based on our results with no significant differences, we

concluded that we might need to validate the protocol of the assay and the counting method.

Finally, we optimized the apoptosis assay for cervical cancer cells since it was the first time at the radiobiology lab that this assay was applied for adherent cell lines. The apoptosis assay allowed us to study the induction of cell death (apoptosis) in cancer cells after therapy. A first trial with normal trypsinization, lead to high levels of apoptosis detected in healthy cells (data not shown). Hence, we first investigated which detachment method would be optimal. We selected a lower concentration of trypsin (0.5x) and compared it so a less invasive detachment enzyme accutase. No significant difference could be seen between the accutase and trypsin (0.5x). However, since the mean of the total amount of apoptotic cells was 1.68 percentage lower with 0.5x trypsin compared to accutase, we applied trypsin 0.5x as the detachment method in our future experiments. The second step was the creation of a template from comparing single and/or double annexin and PI within healthy and dead cells, which were achieved by placing cells in 70℃ for 10 minutes.

We noticed that the time of trypsinization and time for counting the cells had a big effect on the apoptotic numbers and the variation of the data. So, to prevent this, we decided not to count the cells anymore, which clearly decreased the variation of the data. In addition, it is ideal to perform all therapeutic conditions within 1 experiment to limit the variation of the data. From Table 16, it can be seen that the number of living cells decreased when cells were treated with GI but the decrease was not statistically different. However, some p-values were borderline ($p = 0.0571$), showing clearly some trends: control > 2 Gy + GI and control > 8 Gy + GI for the number of living cells, control < 2 Gy + GI for early apoptosis, control < 8 Gy + GI for late apoptosis. Also, the amount of apoptosis was borderline significantly different between control vs 2 Gy + GI and control vs 8 Gy + GI. Interestingly, a trend was seen to increased apoptosis of Hela cells when control was compared to 2 Gy + GI and also with 8Gy + GI, which was not visible when control was compared with 2 Gy only, showing a potential radiosensitizing effect (p 0.0517). However, when 2 Gy was compared to 2 Gy + GI and 8 Gy + GI with 8 Gy,

no significant differences were seen in the amount of living or early, late or mean apoptotic cells, contradicting this statement.

Based on the theory of action of ADAM10 by Liu et al., (2015), migration, invasion, cell proliferation and apoptosis should be affected by ADAM10 inhibition, by preventing the sheddase action of ADAM10. It is also important to note from other studies that ADAM10 may have biological effects than can differ between different types of cancer. For example, in melanoma and bladder carcinoma, the inhibition of ADAM10 prevented cell migration and cell growth. In contrast, in breast cancer, GI showed an effect on migration and invasion but no effect on cell proliferation (Fu et al., 2014, Lee et al., 2010, Gaida et al., 2010, Mullooly et al., 2016). However, in this study, we only saw an effect on cervical cancer cell migration but not on apoptosis and invasion. An anti-migration effect of the GI drug on Hela cervical cancer cells was also shown by Wagiet, (2016).

The idea of ADAM10 playing a part in the invasion and apoptosis of cancer cells was noted by Liu et al., (2015) and Wagiet, (2016) but could not be confirmed in our study. In Jurkat cells, GI induced apoptosis, which seemed to be a result of blocking Notch activation which was not achieved in this experiment (Mullooly et al., 2016). Purow (2009) also found that deregulation of the Notch signaling pathway could cause the suppression of cancer, which was seen in skin cancer, B cell malignancies and non-small cell lung cancer (Mullooly et al., 2016, Purow, 2009).

5.2. Conclusion

We successfully optimized the migration, apoptosis and invasion assay for the Hela and C33A cervical cancer cells. Based on our results, inhibition of ADAM10 with GI254023X lead to decreased migration rate of the Hela cervical cancer cells but did not have an effect on apoptosis and invasion. Combined therapy of GI and RT also had no increased inhibitory effects compared to single therapy. Therefore, we could not conclude that GI254023X functions as a radiosensitizer for cervical cancer. Further testing is required with a larger number of repeats to verify our results.

References

AL JISHI, T. & SERGI, C. 2017. Current perspective of diethylstilbestrol (DES) exposure in mothers and offspring. *Reproductive Toxicology,* 71**,** 71-77.

ANTABE, R. & MKANDAWIRE, P. 2020. HIV/AIDS in Developing Countries. *In:* KOBAYASHI, A. (ed.) *International Encyclopedia of Human Geography (Second Edition).* Oxford: Elsevier.

BAILAR, J. C. & GORNIK, H. L. 1997. Cancer undefeated. *New England Journal of Medicine,* 336**,** 1569-1574.

BANERJEE, R. & KAMRAVA, M. 2014. Brachytherapy in the treatment of cervical cancer: a review. *International journal of women's health,* 6**,** 555-564.

BAZZONI, R. & BENTIVEGNA, A. 2019. Role of Notch Signaling Pathway in Glioblastoma Pathogenesis. *Cancers,* 11**,** 292.

BHATLA, N., BEREK, J. S., CUELLO FREDES, M., DENNY, L. A., GRENMAN, S., KARUNARATNE, K., KEHOE, S. T., KONISHI, I., OLAWAIYE, A. B., PRAT, J. & SANKARANARAYANAN, R. 2019. Revised FIGO staging for carcinoma of the cervix uteri. *International Journal of Gynecology & Obstetrics,* 145**,** 129-135.

BLELOCH, D. J. 2020. Clongenic assay:what,why and how.

BUGAJ, L., SABNIS, A., MITCHELL, A., GARBARINO, J., TOETTCHER, J., BIVONA, T. & LIM, W. 2018. Cancer mutations and targeted drugs can disrupt dynamic signal encoding by the Ras-Erk pathway. *Science,* 361**,** eaao3048.

BURGER, E. A., KIM, J. J., SY, S. & CASTLE, P. E. 2017. Age of Acquiring Causal Human Papillomavirus (HPV) Infections: Leveraging Simulation Models to Explore the Natural History of HPV-induced Cervical Cancer. *Clinical Infectious Diseases,* 65**,** 893-899.

CANCSA 2016. Fact Sheet and Position Statement on Cervical Cancer.

CATARINO, R., PETIGNAT, P., DONGUI, G. & VASSILAKOS, P. 2015. Cervical cancer screening in developing countries at a crossroad: Emerging technologies and policy choices. *World journal of clinical oncology,* 6**,** 281.

CAVICCHI, R. E., COLLETT, C., TELIKEPALLI, S., HU, Z., CARRIER, M. & RIPPLE, D. C. 2017. Variable Threshold Method for Determining the Boundaries of Imaged Subvisible Particles. *Journal of pharmaceutical sciences,* 106**,** 1499-1507.

CHEN, X., JIANG, J., SHEN, H. & HU, Z. 2011. Genetic susceptibility of cervical cancer. *Journal of biomedical research,* 25**,** 155-164.

CHEVARIE-DAVIS, M. & FRANCO, E. 2013. Chapter 78 - Vaccination and Screening in Cervical Cancer Control and Prevention. *In:* GOLDMAN, M. B., TROISI, R. & REXRODE, K. M. (eds.) *Women and Health (Second Edition).* Academic Press.

COLLECTION, T. A. T. C. 2020. American Type Culture Collection.

CRAFTON, S. M. & SALANI, R. 2016. Beyond chemotherapy: an overview and review of targeted therapy in cervical cancer. *Clinical therapeutics,* 38**,** 449-458.

CRAWFORD, H. C., DEMPSEY, P. J., BROWN, G., ADAM, L. & MOSS, M. L. 2009. ADAM10 as a therapeutic target for cancer and inflammation. *Current pharmaceutical design,* 15**,** 2288-2299.

CREE, A., LIVSEY, J., BARRACLOUGH, L., DUBEC, M., HAMBROCK, T., VAN HERK, M., CHOUDHURY, A. & MCWILLIAM, A. 2018. The Potential Value of MRI in External-Beam Radiotherapy for Cervical Cancer. *Clinical Oncology,* 30**,** 737-750.

DAHIYA, N., ACHARYA, A. S., BACHANI, D. & GOEL, M. K. 2016. Strategies for reducing risk of cervical cancer in adolescents in developing countries – A view point. *Indian Journal of Medical Specialities,* 7**,** 35-38.

DENNY, L. 2010. Cervical cancer in South Africa: an overview of current status and prevention strategies. *Continuing Medical Education,* 28.

DUAN, J. X., RAPTI, M., TSIGKOU, A. & LEE, M. H. 2015. Expanding the Activity of Tissue Inhibitors of Metalloproteinase (TIMP)-1 against Surface-Anchored Metalloproteinases by the Replacement of Its C-Terminal Domain: Implications for Anti-Cancer Effects. *PLOS ONE,* 10**,** e0136384.

DUENAS-GONZALEZ, A., SERRANO-OLVERA, A., CETINA, L. & CORONEL, J. 2014. New molecular targets against cervical cancer. *International journal of women's health,* 6**,** 1023.

DUFFY, M. J., MULLOOLY, M., O'DONOVAN, N., SUKOR, S., CROWN, J., PIERCE, A. & MCGOWAN, P. M. 2011. The ADAMs family of proteases: new biomarkers and therapeutic targets for cancer? *Clinical Proteomics,* 8**,** 9.

FU, L., LIU, N., HAN, Y., XIE, C., LI, Q. & WANG, E. 2014. ADAM10 regulates proliferation, invasion, and chemoresistance of bladder cancer cells. *Tumor Biology,* 35**,** 9263-9268.

GAIDA, M. M., HAAG, N., GÜNTHER, F., TSCHAHARGANEH, D. F., SCHIRMACHER, P., FRIESS, H., GIESE, N. A., SCHMIDT, J. & WENTE, M. N. 2010. Expression of A disintegrin and metalloprotease 10 in pancreatic carcinoma. *International journal of molecular medicine,* 26**,** 281-288.

GENOMES PROJECT, C., AUTON, A., BROOKS, L. D., DURBIN, R. M., GARRISON, E. P., KANG, H. M., KORBEL, J. O., MARCHINI, J. L., MCCARTHY, S., MCVEAN, G. A. & ABECASIS, G. R. 2015. A global reference for human genetic variation. *Nature,* 526**,** 68-74.

GERSEY, Z., OSIASON, A. D., BLOOM, L., SHAH, S., THOMPSON, J. W., BREGY, A., AGARWAL, N. & KOMOTAR, R. J. 2019. Therapeutic Targeting of the Notch Pathway in Glioblastoma Multiforme. *World neurosurgery,* 131**,** 252-263. e2.

GONG, L., ZHANG, Y., LIU, C., ZHANG, M. & HAN, S. 2021. Application of Radiosensitizers in Cancer Radiotherapy. *International journal of nanomedicine,* 16**,** 1083-1102.

GRAY, M., TURNBULL, A. K., WARD, C., MEEHAN, J., MARTÍNEZ-PÉREZ, C., BONELLO, M., PANG, L. Y., LANGDON, S. P., KUNKLER, I. H., MURRAY, A. & ARGYLE, D. 2019. Development and characterisation of acquired radioresistant breast cancer cell lines. *Radiation Oncology,* 14**,** 64.

GUPTA, S. 2019. Adjuvant chemotherapy in locally advanced cervical cancer: the ceiling remains unbroken. *Journal of gynecologic oncology,* 30**,** e97-e97.

HANAHAN, D. & WEINBERG, R. A. 2000. The hallmarks of cancer. *Cell,* 100**,** 57-70.

HANAHAN, D. & WEINBERG, R. A. 2011. Hallmarks of cancer: the next generation. *Cell,* 144**,** 646-74.

HEALTH, N. D. O. 2017. Cervical cancr prevention and control policy.

HEIN, A. L., OUELLETTE, M. M. & YAN, Y. 2014. Radiation-induced signaling pathways that promote cancer cell survival (Review). *Int J Oncol,* 45**,** 1813-1819.

HILAL, Z. H., FRANZISKA DOGAN, ASKIN CETIN, C. E. M. KRENTEL, HARALD SCHIERMEIER, SVEN SCHULTHEIS, BEATE TEMPFER, CLEMENS B. 2016. Lymphoma of the Cervix: Case Report and Review of the Literature. *Anticancer Research,* 26**,** 4931.

HUANG, R. & ROFSTAD, E. K. 2017. Cancer stem cells (CSCs), cervical CSCs and targeted therapies. *Oncotarget,* 8**,** 35351-35367.

IBEANU, O. A. 2011. Molecular pathogenesis of cervical cancer. *Cancer biology & therapy,* 11**,** 295-306.

JADON, R., PEMBROKE, C. A., HANNA, C. L., PALANIAPPAN, N., EVANS, M., CLEVES, A. E. & STAFFURTH, J. 2014. A Systematic Review of Organ Motion and Image-guided Strategies in External Beam Radiotherapy for Cervical Cancer. *Clinical Oncology,* 26**,** 185-196.

JUANES, M. A., FEES, C. P., HOEPRICH, G. J., JAISWAL, R. & GOODE, B. L. 2020. EB1 directly regulates APC-mediated actin nucleation. *Current Biology,* 30**,** 4763-4772. e8.

KAHL, D. R. Z. D. V. 2020. *Wound Healing FastTrack AI Image Analysis* [Online]. . Available: https://ibidi.com/img/cms/resources/AG/FL_AG_033_Wound_Healing_150dpi.pdf [Accessed].

KALYANARAMAN, B. 2017. Teaching the basics of cancer metabolism: Developing antitumor strategies by exploiting the differences between normal and cancer cell metabolism. *Redox biology,* 12**,** 833-842.

KATO, T., HAGIYAMA, M. & ITO, A. 2018. Renal ADAM10 and 17: Their Physiological and Medical Meanings. *Frontiers in Cell and Developmental Biology,* 6.

KHAN, S. R., ROCKALL, A. G. & BARWICK, T. D. 2016. Molecular imaging in cervical cancer. *The Quarterly Journal of Nuclear Medicine and Molecular Imaging: Official Publication of the Italian Association of Nuclear Medicine (AIMN)[and] the International Association of Radiopharmacology (IAR),[and] Section of the Society of...* 60**,** 77-92.

KIRISITS, C., LANG, S., DIMOPOULOS, J., BERGER, D., GEORG, D. & PÖTTER, R. 2006. The Vienna applicator for combined intracavitary and interstitial brachytherapy of cervical cancer: design, application, treatment planning, and dosimetric results. *International Journal of Radiation Oncology* Biology* Physics,* 65**,** 624-630.

KLEIN, E., HELZNER, E., SHAYOWITZ, M., KOHLHOFF, S. & SMITH-NOROWITZ, T. A. 2018. Female genital mutilation: health consequences and complications—a short literature review. *Obstetrics and gynecology international,* 2018.

KOCH, C. J., PARLIAMENT, M. B., BROWN, J. M. & URTASUN, R. C. 2010. 4 - Chemical Modifiers of Radiation Response. *In:* HOPPE, R. T., PHILLIPS, T. L. & ROACH, M. (eds.) *Leibel and Phillips Textbook of Radiation Oncology (Third Edition).* Philadelphia: W.B. Saunders.

KUHLE, C. L., ZHANG, X. & KAPOOR, E. Misconceptions about sexual health in older women: why we need to talk about it. Mayo Clinic Proceedings, 2021. Elsevier, 866-869.

L'ANNUNZIATA, M. F. 2016. Chapter 1 - Radioactivity and Our Well-Being. *In:* L'ANNUNZIATA, M. F. (ed.) *Radioactivity (Second Edition).* Boston: Elsevier.

LAMBERTI, G., ANDRINI, E., SISI, M., FEDERICO, A. D. & RICCIUTI, B. 2020. Targeting DNA damage response and repair genes to enhance anticancer immunotherapy: rationale and clinical implication. *Future Oncology,* 16**,** 1751-1766.

LAPRESA, M., PARMA, G., PORTUESI, R. & COLOMBO, N. 2015. Neoadjuvant chemotherapy in cervical cancer: an update. *Expert review of anticancer therapy,* 15**,** 1171-1181.

LEE, S. B., SCHRAMME, A., DOBERSTEIN, K., DUMMER, R., ABDEL-BAKKY, M. S., KELLER, S., ALTEVOGT, P., OH, S. T., REICHRATH, J. & OXMANN, D. 2010. ADAM10 is upregulated in melanoma metastasis compared with primary melanoma. *Journal of Investigative Dermatology*, 130**,** 763-773.

LI, F., ZHOU, K., GAO, L., ZHANG, B., LI, W., YAN, W., SONG, X., YU, H., WANG, S. & YU, N. 2016a. Radiation induces the generation of cancer stem cells: A novel mechanism for cancer radioresistance. *Oncology letters*, 12**,** 3059-3065.

LI, H., WU, X. & CHENG, X. 2016b. Advances in diagnosis and treatment of metastatic cervical cancer. *Journal of gynecologic oncology*, 27**,** e43-e43.

LI, K., TAY, F. R. & YIU, C. K. Y. 2020. The past, present and future perspectives of matrix metalloproteinase inhibitors. *Pharmacology & therapeutics*, 207**,** 107465.

LIGHTFOOT, M., MONTEMORANO, L. & BIXEL, K. 2020. PARP Inhibitors in Gynecologic Cancers: What Is the Next Big Development? *Current Oncology Reports*, 22**,** 29.

LIU, C. & WANG, R. 2019. The roles of hedgehog signaling pathway in radioresistance of cervical cancer. *Dose-Response*, 17**,** 1559325819885293.

LIU, S., ZHANG, W., LIU, K., JI, B. & WANG, G. 2015. Silencing ADAM10 inhibits the in vitro and in vivo growth of hepatocellular carcinoma cancer cells. *Mol Med Rep*, 11**,** 597-602.

MAJIDINIA, M., DARBAND, S. G., KAVIANI, M., NABAVI, S. M., JAHANBAN-ESFAHLAN, R. & YOUSEFI, B. 2018. Cross-regulation between Notch signaling pathway and miRNA machinery in cancer. *DNA Repair*, 66-67**,** 30-41.

MALIEKAL, T., BAJAJ, J., GIRI, V., SUBRAMANYAM, D. & KRISHNA, S. 2008. The role of Notch signaling in human cervical cancer: implications for solid tumors. *Oncogene*, 27**,** 5110-5114.

MARCU, L. G. 2013. Improving therapeutic ratio in head and neck cancer with adjuvant and cisplatin-based treatments. *BioMed research international*, 2013**,** 817279-817279.

MARQUINA, G., MANZANO, A. & CASADO, A. 2018. Targeted Agents in Cervical Cancer: Beyond Bevacizumab. *Current Oncology Reports*, 20**,** 40.

MISHRA, G. A., PIMPLE, S. A. & SHASTRI, S. S. 2011. An overview of prevention and early detection of cervical cancers. *Indian journal of medical and paediatric oncology : official journal of Indian Society of Medical & Paediatric Oncology*, 32**,** 125-132.

MOSS, M. L., STOECK, A., YAN, W. & DEMPSEY, P. J. 2008. ADAM10 as a target for anti-cancer therapy. *Current pharmaceutical biotechnology*, 9**,** 2-8.

MULLOOLY, M., MCGOWAN, P. M., CROWN, J. & DUFFY, M. J. 2016. The ADAMs family of proteases as targets for the treatment of cancer. *Cancer biology & therapy*, 17**,** 870-880.

MUSTAFA, W., ABD HALIM, A., JAMLOS, M. & SYED IDRUS, S. Z. 2020. A Review: Pap Smear Analysis Based on Image Processing Approach. *Journal of Physics: Conference Series*, 1529**,** 022080.

NCI 2021a. Screening and Prevention Editorial Board. PDQ Cervical Cancer Screening. Bethesda, MD: National Cancer

NCI, N. C. I. 2021b. *What is cancer?* [Online]. NCI. Available: https://www.cancer.gov/about-cancer/understanding/what-is-cancer [Accessed July 2021].

OJOVAN, M. I., LEE, W. E. & KALMYKOV, S. N. 2019. Chapter 4 - Naturally Occurring Radionuclides. *In:* OJOVAN, M. I., LEE, W. E. & KALMYKOV, S. N. (eds.) *An Introduction to Nuclear Waste Immobilisation (Third Edition).* Elsevier.

OLIVARES-URBANO, M. A., GRIÑÁN-LISÓN, C., MARCHAL, J. A. & NÚÑEZ, M. I. 2020. CSC Radioresistance: A Therapeutic Challenge to Improve Radiotherapy Effectiveness in Cancer. *Cells,* 9**,** 1651.

OLPIN, J., CHUANG, L., BEREK, J. & GAFFNEY, D. 2018. Imaging and cancer of the cervix in low- and middle-income countries. *Gynecologic oncology reports,* 25**,** 115-121.

PALMEIRA-DE-OLIVEIRA, R., DUARTE, P., PALMEIRA-DE-OLIVEIRA, A., DAS NEVES, J., AMARAL, M. H., BREITENFELD, L. & MARTINEZ-DE-OLIVEIRA, J. 2014. What do Portuguese women prefer regarding vaginal products? Results from a cross-sectional web-based survey. *Pharmaceutics,* 6**,** 543-556.

PALMISANO, R. & ITOH, Y. 2010. Analysis of MMP-Dependent Cell Migration and Invasion. *In:* CLARK, I. M. (ed.) *Matrix Metalloproteinase Protocols.* Totowa, NJ: Humana Press.

PARKIN, E. & HARRIS, B. 2009. A disintegrin and metalloproteinase (ADAM)-mediated ectodomain shedding of ADAM10. *Journal of neurochemistry,* 108**,** 1464-1479.

PUROW, B. 2009. Notch inhibitors as a new tool in the war on cancer: a pathway to watch. *Current pharmaceutical biotechnology,* 10**,** 154-160.

QIN, C., CHEN, X., BAI, Q., DAVIS, M. R. & FANG, Y. 2014. Factors associated with radiosensitivity of cervical cancer. *Anticancer research,* 34**,** 4649-4656.

RECZEK, C. R. & CHANDEL, N. S. 2017. The Two Faces of Reactive Oxygen Species in Cancer. *Annual Review of Cancer Biology,* 1**,** 79-98.

REISS, K. & SAFTIG, P. The "a disintegrin and metalloprotease"(ADAM) family of sheddases: physiological and cellular functions. Seminars in cell & developmental biology, 2009. Elsevier, 126-137.

ROCKS, N., PAULISSEN, G., EL HOUR, M., QUESADA, F., CRAHAY, C., GUÉDERS, M., FOIDART, J.-M., NOËL, A. & CATALDO, D. 2008. Emerging roles of ADAM and ADAMTS metalloproteinases in cancer. *Biochimie,* 90**,** 369-379.

RONG, C., FENG, Y. & YE, Z. 2017. Notch is a critical regulator in cervical cancer by regulating Numb splicing. *Oncology letters,* 13**,** 2465-2470.

RYAN, J. L. 2012. Ionizing radiation: the good, the bad, and the ugly. *Journal of Investigative Dermatology,* 132**,** 985-993.

SAAD, M. I., ROSE-JOHN, S. & JENKINS, B. J. 2019. ADAM17: An Emerging Therapeutic Target for Lung Cancer. *Cancers,* 11**,** 1218.

SEEGAR, T. C., KILLINGSWORTH, L. B., SAHA, N., MEYER, P. A., PATRA, D., ZIMMERMAN, B., JANES, P. W., RUBINSTEIN, E., NIKOLOV, D. B. & SKINIOTIS, G. 2017. Structural basis for regulated proteolysis by the α-secretase ADAM10. *Cell,* 171**,** 1638-1648. e7.

SEIFERT, A., DÜSTERHÖFT, S., WOZNIAK, J., KOO, C. Z., TOMLINSON, M. G., NUTI, E., ROSSELLO, A., CUFFARO, D., YILDIZ, D. & LUDWIG, A. 2020. The metalloproteinase ADAM10 requires its activity to sustain surface expression. *Cellular and Molecular Life Sciences*.

SELVAGGI, L., LOIZZI, V., DI GILIO, A., NARDELLI, C., CANTATORE, C. & CORMIO, G. 2006. Neoadjuvant chemotherapy in cervical cancer: a 67 patients experience. *International Journal of Gynecologic Cancer,* 16.

SEVER, R. & BRUGGE, J. S. 2015. Signal transduction in cancer. *Cold Spring Harbor perspectives in medicine,* 5**,** a006098.

SHAFABAKHSH, R., REITER, R. J., MIRZAEI, H., TEYMOORDASH, S. N. & ASEMI, Z. 2019. Melatonin: a new inhibitor agent for cervical cancer treatment. *Journal of cellular physiology,* 234**,** 21670-21682.

SMITH JR, T. M., THARAKAN, A. & MARTIN, R. K. 2020. Targeting ADAM10 in cancer and autoimmunity. *Frontiers in immunology,* 11**,** 499.

STOLNICU, S. H., LIEN HANKO-BAUER, ORSOLYA BARSAN, IULIA TERINTE, CRISTINA PESCI, ANNA AVIEL-RONEN, SARIT KIYOKAWA, TAKAKO ALVARADO-CABRERO, ISABEL OLIVA, ESTHER PARK, KAY J. SOSLOW, ROBERT A. 2019. Cervical adenosquamous carcinoma: detailed analysis of morphology, immunohistochemical profile, and clinical outcomes in 59 cases. *Modern pathology : an official journal of the United States and Canadian Academy of Pathology, Inc,* 32**,** 269.

SU, W.-H., CHUANG, P.-C., HUANG, E.-Y. & YANG, K. D. 2012. Radiation-induced increase in cell migration and metastatic potential of cervical cancer cells operates via the K-Ras pathway. *The American journal of pathology,* 180**,** 862-871.

SUN, R., CHEN, C., DENG, X., WANG, F., SONG, S., CAI, Q., WANG, J., ZHANG, T., SHI, M. & KE, Q. 2021. IL-11 mediates the Radioresistance of Cervical Cancer Cells via the PI3K/Akt Signaling Pathway. *Journal of Cancer,* 12**,** 4638.

SUWA, T., KOBAYASHI, M., NAM, J.-M. & HARADA, H. 2021. Tumor microenvironment and radioresistance. *Experimental & Molecular Medicine,* 53**,** 1029-1035.

TAPERA, O., DREYER, G., KADZATSA, W., NYAKABAU, A., STRAY-PEDERSEN, B. & HENDRICKS, S. 2019. Cervical cancer knowledge, attitudes, beliefs and practices of women aged at least 25 years in Harare, Zimbabwe. *BMC women's health,* 19**,** 1-10.

TEAM, A. C. S. M. A. E. C. 2020a. Cervical cancer early detection, diagnosis and staging.

TEAM, T. A. C. S. 2020b. *American Cancer Society* [Online]. Available: https://www.cancer.org/cancer/cervical-cancer/about/what-is-cervical-cancer.html#references [Accessed].

TITUS, L., HATCH, E. E., DRAKE, K. M., PARKER, S. E., HYER, M., PALMER, J. R., STROHSNITTER, W. C., ADAM, E., HERBST, A. L., HUO, D., HOOVER, R. N. & TROISI, R. 2019. Reproductive and hormone-related outcomes in women whose mothers were exposed in utero to diethylstilbestrol (DES): A report from the US National Cancer Institute DES Third Generation Study. *Reproductive Toxicology,* 84**,** 32-38.

TROISI, R., HATCH, E. E., TITUS-ERNSTOFF, L., HYER, M., PALMER, J. R., ROBBOY, S. J., STROHSNITTER, W. C., KAUFMAN, R., HERBST, A. L. & HOOVER, R. N. 2007. Cancer risk in women prenatally exposed to diethylstilbestrol. *International journal of cancer,* 121**,** 356-360.

UNIVERISITY, E. 2018. *How Cancer Spreads (Metastasis)* [Online]. Available: https://www.cancerquest.org/cancer-biology/metastasis#toc-overview-o-UYPadeTt [Accessed].

VORDERMARK, D. 2016. Radiotherapy of cervical cancer. *Oncology research and treatment,* 39**,** 516-520.

WAGIET, M. 2016. *Modulating ADAM-10 activity and expression in cervical and oesophageal cancer cells.* University of Cape Town.

WALLER, V. & PRUSCHY, M. 2021. Combined Radiochemotherapy: Metalloproteinases Revisited. *Front Oncol,* 11**,** 676583.

WARDAK, S. 2016. Human Papillomavirus (HPV) and cervical cancer. *Medycyna doswiadczalna i mikrobiologia,* 68**,** 73-84.

WEINBERG, R. A. 1996. How cancer arises. *Scientific American,* 275**,** 62-70.

WETZEL, S., SEIPOLD, L. & SAFTIG, P. 2017. The metalloproteinase ADAM10: A useful therapeutic target? *Biochimica et Biophysica Acta (BBA) - Molecular Cell Research,* 1864**,** 2071-2081.

WHITE, M. C., HOLMAN, D. M., BOEHM, J. E., PEIPINS, L. A., GROSSMAN, M. & HENLEY, S. J. 2014. Age and cancer risk: a potentially modifiable relationship. *American journal of preventive medicine,* 46**,** S7-S15.

WHO 2021. WHO guideline for screening and treatment of cervical pre-cancer lesions for cervical cancer prevention. World Health Organization, ed.

YAHYANEJAD, S., THEYS, J. & VOOIJS, M. 2016. Targeting Notch to overcome radiation resistance. *Oncotarget,* 7**,** 7610.

YU, S. D., LIU, F. Y. & WANG, Q. R. 2012. Notch inhibitor: a promising carcinoma radiosensitizer. *Asian Pac J Cancer Prev,* 13**,** 5345-51.